Radiative Quenching of Hydrogen Molecular Ion in 2 Dimensions

by

Želimir Lučić

Bachelor of Science University of Sarajevo 1991
Master of Engineering Simon Fraser University 2002
Master of Applied Science University of Washington 2010

A dissertation submitted in partial fulfillment
of the requirements for the
Doctor of Philosophy – Physics

advisor Dr. Bernard Zygelman

Department of Physics
College of Sciences
Graduate College
University of Nevada, Las Vegas

Acknowledgments

First I would like to thank my supervisor, Dr. Bernard Zygelman, for all his help and advice.

Thanks to the usual suspects, my parents and my sister, for their help.

I would also like to thank all my friends, who asked questions about this thesis and made me guilty for not completing it on time.

Thesis advisor: Professor Dr. Bernard Zygelman Zelimir Lucic

Radiative Quenching of Hydrogen Molecular Ion in 2 Dimensions

Abstract

The goal of this thesis is twofold. First it is to present and investigate the hydrogen molecular ion in the 2 dimensions where the motivation is the applications of the 2 dimensional matherials. The second goal is to analyze and calculate, in 2 dimensions, the radiative quenching cross section of the hydrogen ion molecule.

Contents

Listing of figures

CHAPTER 1

INTRODUCTION

1.1 MOTIVATION

For a long time humanity asked itself about the origin of the universe, its final destiny, origin and possible evolution of its laws and humanity place in all of those. Not being able to answer any of those questions,

Arguably, quantum mechanics (QM), or the quantum theory, offers the best description of matter's behavior at the atomic, molecular, and sub-nuclear levels. As an established paradigm, it is increasingly applied to increasingly more complex systems where physics and other disciplines intersect.

QM has increasingly found applications in information theory, material, and the life sciences, areas that traditionally used to lie in the domain of classical physics. Within information theory, a new computing paradigm is emerging. It is recognized that the quantum theory allows the processing of information[?] not available within the classical framework. The principles of QM have en-

abled a novel and powerful information processing platform, quantum computing. The latter's basic component is called a qubit[?] and is the quantum analog of the bit, the lowest common denominator of classical information. Qubits are fragile in that quantum coherence, which gives the quantum computer its power, requires a noise-free environment that is difficult to establish and maintain in the laboratory. Several platforms for qubit technologies have been explored, including trapped ions and superconducting circuits[?] . At present, it is not known if present-day qubit technologies can be scaled to build a functional and useful quantum computer.

One promising platform, topological quantum computing[?,?,?,?,?] , relies on the unusual quantum properties of 2-dimensional (2D) matter. In the past few decades, there have been great strides in creating 2D materials that promise novel applications.[?] To facilitate this emergent technology, it is imperative that we understand, at a fundamental level, the processes that govern the behavior of matter at the atomic and molecular levels. In this thesis, we will explore ions' interactions with the neutral matter in a 2D environment. Specific topics include radiative quenching, non-radiative and radiative charge transfer reactions, and the manipulation and control of atomic matter by external fields. Such processes are important in 3D gases, as in astrophysical and laboratory plasma environments, and have attracted much attention[?]

However, there have been relatively few studies concerning charge transfer processes in 2D.

In this thesis, we will calculate the rate of the radiative and charge transfer reactions between a positively charged ion and neutral 2D hydrogen at very low collision energies. In our formalism, the particles are constrained to move in a 2D manifold, but the emitted radiation can propagate in 3D. This study will provide insight into how constrained 2D dynamics affect the rate coefficient for radiative charge transfer. (TODO: Make this sentence reflect the actual work)

1.2 Some Applications of the 2D Quantum Mechanics

Quantum Mechanics was developed during the first quarter of the 20th century, and its methods have been applied to increasingly complex systems. QM has allowed the development of novel electronic components, lasers, high-speed telecommunications, new diagnostic technologies in medicine, and new materials.

In this introduction, we discuss two major applications. One is a creation of the novel, 2-dimensional materials. The second is the application of 2D materials to quantum computing.

1.2.1 New Materials

The application of QM to solid-state systems has led to a deeper understanding of the properties of materials. That understanding has led to the creation of new materials, including so-called two-dimensional (2D) materials.

2D materials can exhibit unique topological properties that do not exist in the 3D case. An exciting and important feature in this context is the emergence of anyons[?]. Anyons are neither Fermions nor Bosons. The exchange of two anyons induces an arbitrary relative phase between the partners; an effect called fractional statistics. In 3D space, the relative phase can only take the integer values of 2π (Bosons) or π (Fermions).

1.2.2 On 2D Material No-Go Theorems and Graphene

Landau and Pierls[? ?] initially argued that 2D materials could not exist. That argument posited that the displacement of atoms at finite temperatures induces thermal fluctuations that are an order of the atomic distance and lead to melting of the 2D material at temperatures higher than $0K$.

There is an even stronger statement against 2D materials, in the form of the Mermin-Wagner-Hohenberg (MWH) theorem[? ?]. In these papers, the authors show that 2D systems with short-range interactions are unstable and cannot exist. Using thermodynamics arguments, one can show that a 3D system is stable if its free energy is bounded from below and convex (upwards). In this way, the system can minimize the energy of the ground state. Because higher-order fluctuations are finite, the system is stable. The MWH argument posits that, in 2D systems, fluctuations around the ordered state (lattice in the 2D case) decorrelate over large distances, thus destroying the large-scale order. Therefore, it seemed that the possible existence and applications of the 2D materials were quite limited. The only 2D materials considered stable were

thin molecular films, which could form on a solids' surface. Dash[?] predicts that 2D materials exist as a thin film either on the surface of the boundaries of 3D materials.

Despite those arguments, it has been speculated that stable 2D materials are possible[?]. The situation changed dramatically in 2004 when 2D carbon (Graphene) was discovered and created in the laboratory[??] at the University of Manchester, Great Britain.

2D materials have qualitatively different topological properties[?]. Moreover, those properties do not depend on the type of microscopic interactions between particles. While this subject is beyond the scope of this thesis, it does show that the field of 2D materials is a fertile ground for both fundamental and applied research. Interestingly, it has been shown[?] that it takes ten layers of Graphene for it to start behaving like a 'regular' 3D material. The existence of graphene does not contradict the above-mentioned no-go theorem[?], but it does circumvent it[?]. In graphene, thermal oscillations produce ripples or bending of the graphene sheet. That way, graphene behaves like an elastic membrane that allows phonons to propagate in 2 dimensions and couple in a plane stretching along the transverse fluctuations out of the plane. These phonons mediate a long-range interaction, thereby circumventing the Mermin-Wagner no-go theorem.

Additionally[?],2D materials exhibit several other interesting properties. Its quantum excitations behave in a manner described by relativistic dynamics.

Usually, in condensed matter systems, the Schrodinger equation's solutions describe the material's electronic properties. In graphene, the electrons obey the non-relativistic Schrodinger equation, but interactions with the graphene lattice's periodic potential give rise to solutions referred to as quasiparticles excitations, and they behave in the same manner as massless Dirac fermions. Even at low energies, these quasiparticles are described by a Dirac equation in 2+1 dimensions.

Additionally[? ?] ,2D materials exhibit several other exciting properties. Its quantum excitations behave in a manner described by relativistic dynamics. Usually, in condensed matter systems, the Schrodinger equation's solutions describe the material's electronic properties. In graphene, electrons obey the non-relativistic Schrodinger equation. Still, interactions with the graphene lattice's periodic potential give rise to solutions referred to as quasiparticles excitations, and they behave in the same manner as massless Dirac fermions. Even at low energies, these quasiparticles are described by a Dirac equation in 2+1 dimensions.[?]

1.2.3 EXCITONS

These excitations represent a wide class of intrinsic electronic excitations (Excitons)[? ?] in crystals of semiconductors and dielectrics. In one model, Excitons represent a bound state of an electron and a hole, typically formed when an incident photon is absorbed, exciting an electron from the valence to the conduction band. The attractive Coulomb interaction between the excited

electron and the newly created hole binds them together to form a bound neutral compound system of the two charge carriers similar to a hydrogen atom. The character of exciton motion depends on the strength of the exciton interaction with phonons. The electron-hole model is common in crystals of insulators and semiconductors. Ya. I. Frenkel (1931) create excitons to explain the light absorption in crystals, which does not lead to photoconductivity. In the Frenkel model, the exciton is considered as an electronic excitation of one crystal site with the energy close to, but a bit smaller than that necessary for the excitation of a free electron. Due to the crystal's translation symmetry, the exciton can move along the lattice sites transferring the energy to the electrically active or luminescence centers.

Similar excitations occur in 2D systems.[??] . The 2D excitons promise to form a building block of the 2D electronics.[?] . Although exciton-based transistor actions have been demonstrated successfully in bulk semiconductor-based coupled quantum wells, the low temperature required for their operation limits their practical application. The emergence of 2D semiconductors with large exciton binding energies may lead to excitonic devices and circuits that operate at room temperature.[?] .

Therefore, it might be interesting to redo the same calculation as we did but solving Dirac's equation for the system of quasiparticles similar to a hydrogen ion.

1.2.4 GRAPHENE

Graphene exhibits similar properties[?], such as its Quantum Electrodynamics (QED) like electronic spectrum, electron tunneling. Another interesting consequence of the QED like electron spectrum is the possibility of experimentally studying QED in curved space by controllable bending of a graphene sheet. Such study may offer a possibility to address a certain class of cosmological problems.

At present, since the discovery of graphene, several new 2D materials have been identified[?]. As the new 2D materials are getting discovered, people are investigating their possible applications. One of the very useful applications for any exotic materials is electronics. These new 2D materials promise that they can be used to build existing electronic components, but with potentially better performances[? ?].

Nanotubes are rolled-up graphene sheets, and depending on the application, graphene (as a sheet) is sometimes superior, sometimes inferior, and sometimes completely different. The other fascinating application is the appearance of high-temperature superconductivity in 2D materials[?].

2D ELECTRONICS

Driven by a demand for higher performance and lower consumption in electronic devices, 2D materials have found application in that arena[?,?]. There is the hope that Graphene can be used to build active electronic components,

such as diodes, transistors (FET), and other electronic components. Alternatively, Graphene may also be used as a conductor in electronic components and batteries due to its conductivity. Graphene itself is a zero-gap semiconductor. There is another unique opportunity in 2D semiconductors. In a 3D semiconductor, electronic states are buried deep inside the material. Unlike the surface state, electron states inside the material are localized, i.e., the wave function has an exponentially decaying tail.

In 2D semiconductors, the electronic states exist on the surface. The surface states admit both localized and non-localized, Block bulk states[?] . Another interesting application of 2D electronics is the LED elements in 2D[?] . The electronics research is closely related to the research of new 2D materials. For example, Graphene itself is not compatible with silicon. However, there is a new material, black phosphorus[?] , which is both compatible with silicon and it holds promise for future electronic[?] devices. This fact relies on two key properties; the first is that black phosphorus has higher mobility, the speed at which it can carry an electrical charge, than silicon. The other is that it has a finite bandgap, whereas Graphene does not. So, in essence, in the presence of an electric field, black phosphorus can act as a semiconductor[?] .

QUANTUM COMPUTING

The current computer architecture is based on the so-called 'von Neumann' architecture. The algorithms based on that architecture have some inherent limits, and as it currently stands, the architecture cannot overcome those lim-

its.

There are two main classes of computer algorithms, P and NP. There are subclasses within those classes, but those two classes capture the essential behavior of classical algorithms. The algorithms belonging to class P are solvable in polynomial time, with regard to the size of the input. Those algorithms belonging to class NP are those which require exponential time to complete$^?$.

Currently, the major unsolved problem in Computer Science is the P vs. NP problem$^?$. While the hypothesis that $P \neq NP$ is generally accepted, no proof has been found. Applying quantum mechanical principles in engineering disciplines, such as computer science$^?$ promises to bring us the much qualitatively more powerful quantum computer.

Now all problems in the NP class (more precisely, NP-complete subclass) can be transformed into each other in polynomial time to each other$^?$, therefore finding a polynomial-time solution for one of them would amount to having a polynomial-time solution to all problems in NP class. So the goal is rather worthy.

For example, Schor's algorithm$^?$ can provably solve integer factorization in a polynomial time, as opposed to the best classical algorithm (quadratic sieve), which works in sub-exponential time$^?$. Unfortunately, the integer factorization problem, as well as other BQP problems, do not belong to the class of NP-complete problems.

Interestingly, according to Abrams and Lloyd[?],[?] if the small nonlinear term is added to Quantum Mechanics, quantum computers would be able to solve NP-complete problems in polynomial time.

Currently, it is known that the quantum computer will not be able to solve NP problems. They could solve the class of the bounded-error, quantum, polynomial time (BQP) problems[?]. Even if the NP problems remain intractable, just the possibility that according to Feynman[?], a quantum computer can be used to simulate the quantum processes, which will in itself be a step forward.

TOPOLOGICAL QUANTUM COMPUTING

The concept of topological quantum computing[?] depends on the unique properties of 2D materials. In principle, there are no theoretical objections to building a quantum computer; there are serious technical issues, such as noise and scaling limitations, for current qubit technologies that need to be overcome[?]. The topological approach promises a physically realizable quantum computer[?,?].

ANYONS

Anyons are quasi-particles that can arise in 2D systems and whose quantum statistics in neither Fermionic nor Bosonic[?]. This fact has been proven[?], but arbitrary statistics are valid only in 2 dimensions[?]. After exchanging two identical particles, the wave function gains an arbitrary phase factor $\Psi = e^{i\theta}\Psi$, where $\theta = 2\pi\nu^s$. In contrast, for a 3D system, the exchange of two particles

leads to either phase factor π or 0, for fermions and bosons, respectively.

In general, there are two kinds of Anyons, Abelian and non-Abelian. Abelian Anyons have been reliably detected in systems exhibiting the Fractional Quantum Hall Effect[?] . Whereas the computation with Abelian Anyons is theoretically possible[?] , considerably more attention has been paid to non-Abelian Anyons. There are several possibilities for realizing non-abelian statistics experimentally: 1. a two-dimensional electron gas in a large magnetic field (the fractional quantum Hall effect); 2. rapidly rotating Bose-Einstein condensates[?] 3. frustrated magnets[?] . 4. One of the anyons candidates the Majorana fermion[?] . Majorana fermion (particle) the particle that is its own antiparticle. A pair of localized Majorana states has been predicted to reside at the ends of a specially designed superconducting wire. Very recently (2020)[?] there is a strong evidence that Majorana particles has been observed for the first time. The other property of the Majorana fermion is that it is a non-Abelian anyon. This present the possibility for the realization of fault-tolerant topological quantum computing[?] .

EXCITONS AND TRIONS

Other interesting quasiparticle phenomena are called excitons[?] . It is a bound state of a hole and an electron in a solid-state material. Excitons allow the transport of energy without the transport of an electric charge. There are two types of excitons:

1. Frenkel excitons are found in organic molecular crystals[?] and have binding

energies on order of $1eV$ and radii 10Å.

2. Wannier excitons are found in semiconductors[?] and have binding energies on the order of $1meV$ with radii 100Å.

Excitons have been observed in 2D materials[?] as well as 2D excitons in 3D materials. The promise here is that these kinds of quasi-particles can help create a new kind of electronic components, typically opto-electronics.

Since the exciton system resembles either the hydrogen atom or the hydrogen molecule, and it seems conceivable that the dynamics of H_2^+ molecule is qualitatively similar and could be applied to the excitons systems as well.

The similar system is the trion, which consists of either 2 electrons and a hole, or 2 holes and an electron, therefore resembling the hydrogen molecule.

Future Applications and Speculations

While the applications of the 2D materials above are certainly interesting, creating an exact analytical model of such material is extremely complex. Even with today's computing machinery, the many-body wave equation is intractable.

Equations for many bodies systems may formally be created by extending equations for a one or two bodies systems. But as soon as one tries that, one realizes that the complexity of such equations increases enormously, and than assumptions made for a small systems are not valid any more. In this author's opinion, moving from a simple system to an order of magnitude more com-

plex, requires a completely new mathematical and physical framework. Something analogous between the classical mechanics and thermodynamics.

While the 2D materials' applications above are undoubtedly impressive, creating an exact analytical model of such material is too complicated. Even with today's computing machinery, the many-body wave equation is intractable. Equations for many-body systems may formally be created by extending equations for one or two-body systems. But as soon as one tries that, one realizes that such equations' complexity increases enormously and then assumptions made for small systems are no longer valid. In this author's opinion, moving from a simple system to an order of magnitude more complex requires an entirely new mathematical and physical framework—something analogous between classical mechanics and thermodynamics.

OUTLINE

In this thesis, we will focus on investigating and solving the radiative charge transfer TODO: (Reflect actual work) for the most straightforward molecular system, namely hydrogen molecular ion H_2^+ in 2 dimensions (2D in the further text), and solving such system in 2D exactly. Chapter 2 will show that applying our method to the already solved and well-known H_2^+ in 3D yields the same results. Then in chapter 3, we will follow the already well-established procedure[?] to analytically solve the H_2^+. After providing an analytical solution, we will fall back to the numerical methods to calculate the energy levels and obtain the potential curves. In chapter 4, we use the results obtained to cal-

culate such a system's dynamics, namely the Radiate Association process. In chapter 5, we again use the same results to calculate the radiate charge transfer.

In the following chapter, we re-calculate the electron energies for hydrogen molecular ion in 3D by using a different and arguably simpler approach.

We shall use analytic methods where possible and resort to the numerical approach when there is no hope of finding an analytic solution. Quantitative calculations have greatly enabled the advancement of computing technology, as it is now possible to solve partial differential equations relatively quickly using computers that are widely accessible. However, applying approximate methods and using only numerical methods allow limited insights. While the numerical methods provide results, they do not provide much insight into a quantum system's behavior. Furthermore, unless one is cautious, systemic numerical errors can accumulate and lead to neither insightful nor correct results. Therefore, analytic solutions are almost always desirable. However, for moderately complex systems, closed analytic solutions are usually impossible to obtain. Nevertheless, it is still desirable to find an exact analytic solution, if possible, and fall back to numerical methods only as a last step.

Finally, while 2D atoms and molecules do not exist, excitons are proven to exist. So we explore the H_2 molecule so that we gain insights that can be translated into excitons.

CHAPTER 2

HYDROGEN MOLECULAR ION IN 3 DIMENSIONS (3D)

In this chapter, we review analytic methods[? ? ?] used to obtain solutions of the time-independent Schrodinger equation for the hydrogen molecular.

As we will apply a similar method to treat the hydrogen molecular ions in 2D, we first review the methodology of Bates used to calculate the lowest electronic eigenstates and eigenvalues for the H_2^+ system in 3D. *

The hydrogen molecular ion, and similar systems (such as HeH^+) are one of the few that allow a full analytic quantum mechanical description. Although its solutions do not exist in the closed form, they can be expressed as a convergent infinite series. Wasserman in his thesis[?] in 1963 reports that while the existence of H_2^+ has been verified, no discrete spectrum of the H_2^+ has been observed In the same thesis, Wasserman reports that the ionization potential of H_2^+ has been measured and shows good agreement with the theoretical calculations. However, in 1989 Carrington, McNab and Montgomerie re-

*In this section we use atomic (Hatree) units, unless otherwise stated.

port[?] that the radio frequency hyperfine transitions of the H_2^+ have been measured. They note that the H_2^+ is highly reactive and therefore hard to keep in the lab.

As a three-body problem, containing two protons and an electron, the Schrodinger PDE can be separated by expressing it in an elliptical coordinate system. Unfortunately, there does not exist a closed form representation for the eigenvalues and one must resort to numerical methods in their calculation. Bates et al.[? ?] did not provide numerical codes used the evaluation of eigenvalues. Instead, they used an expanded fraction method for calculating the latter with the desired level of precision. The paper[?] does not report on the details of those calculations, and so in this thesis we provide an alternative description. We will compare the results obtained here with those reported in[?] . Harmony with with those reported in[?] will provide confidence in the fidelity of the analogous calculations in 2D.

We use Hartree Atomic Units (2.1), in all equations. In this system the numerical values of the following fundamental constants are 1:

$$\begin{aligned} &\text{Electron mass:} && m_e = 1 \\ &\text{Electron charge:} && e = 1 \\ &\text{Reduced Planck constant:} && \hbar = 1 \\ &\text{Coulomb's constant:} && \frac{1}{4\pi\epsilon_0} = 1 \end{aligned} \tag{2.1}$$

In addition, in equations, variables that represent vectors are typeset either in **bold** or with an arrow above the symbol, $\vec{r}$. A caret $(\hat{})$ above a symbol indi-

cates that the symbol is an operator.

The only place where we specifically will not be using Atomic units will be in the following derivation, where we do transformation of the molecular Hamiltonian into a Jacobian coordinate system. Since some terms will contain reduced mass, we want to keep the units intact.

2.1 DESCRIPTION

The starting point is the Schrodinger equation for the hydrogen molecular ion in 3D. We seek stationary states for non-relativistic motion, and neglect the spin degrees of freedom. With these assumptions the Schrodinger equation for such a system is given by:

$$\hat{H}\psi\left(\mathbf{R},\mathbf{x}\right)=E\,\psi\left(\mathbf{R},\mathbf{x}\right). \tag{2.2}$$

$\hat{H}$ represents total Hamiltonian and $\psi\left(\mathbf{R},\mathbf{x}\right)$ is an eigenstate wavefunction. It is a function of both the collective nuclear coordinates $\mathbf{R}$, and electronic coordinates $\mathbf{x}$. Of course, since we are considering the hydrogen molecular ion, $\mathbf{x}$ is the coordinate of a single electron.

The hydrogen molecular ion H_2^+ is composed of 2 protons and a single electron. Thus, as we are neglecting relativistic effects and spin, its Hamiltonian is given as:

$$\hat{H}=\hat{T}_n+\hat{T}_e+\hat{V}_{en}+\hat{V}_{nn}. \tag{2.3}$$

The terms in the Hamiltonian are as follows:

The kinetic energy of the protons:

$$`\hat{T}_n = -\frac{\hbar^2}{2M}\sum_{i=1}^{2}\nabla_{R_i}^2 = -\frac{1}{2M}\sum_{i=1}^{2}\hat{P}_i^2 \tag{2.4}$$

The kinetic energy of the electron:

$$\hat{T}_e = -\frac{\hbar^2}{2m}\nabla_x^2 = \frac{1}{2m}\hat{p}^2 \tag{2.5}$$

The potential energy between the electron and the nuclei, i.e. the total Coulomb electron - nuclei attraction:

$$\hat{V}_{en} = -\sum_{i=1}^{2}|\mathbf{R}_i - \mathbf{x}| \tag{2.6}$$

Potential energy (operators) between the nuclei - the total Coulomb proton - proton repulsion.

$$\hat{V}_{nn} = \frac{e^2}{|\mathbf{R}_1 - \mathbf{R}_2|} \tag{2.7}$$

The second term in the equation above represents the operator expression.

In the equations above, $\mathbf{R}_i,\ i = 1, 2$ and M represents the coordinates and mass of the nuclei (protons) $1, 2$ respectively, and $\mathbf{x}$ and m are the coordinates and mass of the electron, respectively. Coordinates are defined with respect to a common origin in a space fixed frame.

It is convenient to separate the motion of the center of mass from the motion of the point particles. A similar approach can be applied for the quantum case. We show in Appendix A that the motion of the center of mass will be a plane wave, which possess a well defined momentum and which is not square inte-

grable. That makes the position of the center of mass equally probable in the hole space, which agrees with the Heisenberg uncertainty principle.

In the appendix A we define $\chi(\mathbf{R})$ as the wavefunction representing the motion of the nuclei. We then obtain:

$$\chi(\mathbf{R}) = \frac{1}{(2\pi\hbar)^{3/2}} e^{\frac{i}{\hbar}\sqrt{2ME_{CM}}\mathbf{R}} \tag{2.8}$$

Therefore, we proceed to transform the Hamiltonian into a Jacobian coordinate system, following[?] . The outcome of this procedure will be the transformation of the wave function as $\psi(\mathbf{R}_i, \mathbf{r}) \rightarrow \psi(\mathbf{R}_{CM}, \mathbf{R}, \mathbf{r})$ where the $\mathbf{R}_{CM}$ is the coordinate of the center of the mass, R is the distance between nuclei and $\mathbf{r}$ is an electron coordinate. We choose the coordinates as:

$$\begin{aligned} \mathbf{R}_{CM} &= \frac{M\,\mathbf{R}_1 + M\,\mathbf{R}_2 + m\,\mathbf{x}}{2M+m} \\ \mathbf{R} &= \mathbf{R}_1 - \mathbf{R}_2 \\ \mathbf{r} &= \mathbf{x} - \frac{\mathbf{R}_1 + \mathbf{R}_2}{2} \end{aligned} \tag{2.9}$$

Now following[?] ,[?] , we obtain the expression of the molecular Hamiltonian in

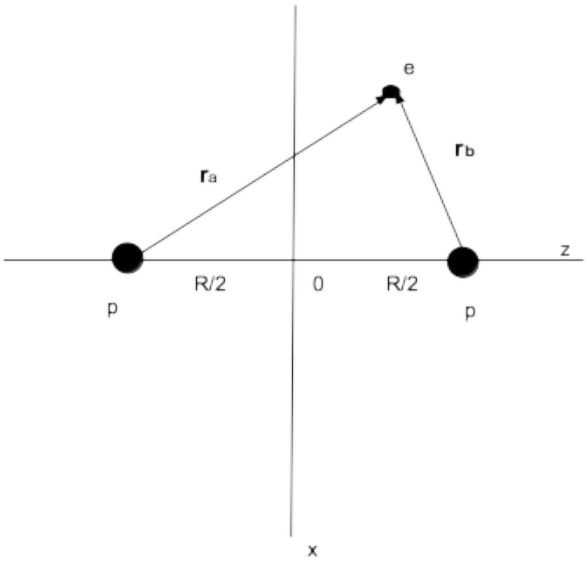

Figure 2.1: H_2 Ion

the new coordinates,

$H^{'} = T_{CM} + T_{KE} + H_{AD}$ where

Motion of the center of the mass which can be separated from the total energy of the nuclei:

$$T_{CM} = -\frac{1}{2(2M+m)}\nabla^2_{CM}$$

The relative motion of the nuclei

$$T_{KE} = -\frac{1}{2\mu}\nabla^2_R$$

where

$\mu = \frac{M}{2}$ is a reduced mass of the 'bare' nuclei

(2.10)

and

The adiabatic Hamiltonian:

$$H_{AD} = -\frac{1}{2m}\nabla^2_r - \frac{1}{4M}\nabla^2_r + \frac{1}{|R|} - \frac{1}{|r+R/2|} - \frac{1}{|r-R/2|} \tag{2.11}$$

The second term $\frac{1}{4M}\nabla^2_r$, in the expression for the H_{AD} represents the mass polarization term, and because $M >> m$, it can be neglected. This term represents the movement of the electron as the center of the mass is moving. In this case the mass polarization is the coupling of the two nuclei, since they are charged and interact with each other. The physical basis for the approximation is the fact that the $m_p \approx 1836 m_e$, where m_p and m_e are the proton's and elec-

tron's mass respectively. Because of the mass difference, the center of the mass (whose mass is mostly mass of the nuclei) is moving much slower than the electron, and thus justifies neglecting this term.

Now we get for the Schrodinger equation:

$$T_{KE}\psi(\mathbf{R},\mathbf{r}) + H_{AD}\psi(\mathbf{R},\mathbf{r}) = E\,\psi(\mathbf{R},\mathbf{r}) \tag{2.12}$$

where E is the internal energy of the nuclei - electron system. To develop a working theory we use Born-Oppenheimer (BO) approximation. Using BO approximation we solve for the electronic Hamiltonian in the Coulomb field of the nuclei, where the nuclei are assumed to be stationary with respect to inertial frame. In this case, the electronic Hamiltonian is the H_{AD} from (2.11). We neglect the mass polarization term and express the electronic Hamiltonian as:

$$\begin{aligned} &H_{AD} = T_e + V_{NN} + V_{Ne} \quad \text{or} \\ &H_{AD} = \frac{1}{2m}\nabla_r^2 + \frac{1}{|R|} - \frac{1}{|r+R/2|} - \frac{1}{|r-R/2|} \end{aligned} \tag{2.13}$$

The BO approximation neglects the motion of the nuclei when describing the electron motion in a molecule. The physical basis for the approximation is the same one as above, $m_p \approx 1836 m_e$. In addition, due to their opposite charges, there is an attractive Coulomb force between proton and electron. But the magnitude of the acceleration is inversely proportional to the mass, so the acceleration of the electron is large and the acceleration of the proton is small, and can be neglected.

So at this step, we neglect the nuclear kinetic energy, effectively rendering the nuclei immobile. Following[?] we then solve for the motion of an electron in the Coulomb field of the nuclei, which leads to a following Schrodinger equation:

$$\left[-\frac{1}{2}\nabla_r^2 + V(\mathbf{R};\mathbf{r})\right] u(\mathbf{R};\mathbf{r}) = E(\mathbf{R})u(\mathbf{R};\mathbf{r}) \tag{2.14}$$

Now the equation (2.14) is the Schrodinger equation for the electron with its coordinate **r** and parameter **R**. Electron is moving in the potential $V(\mathbf{R};\mathbf{r})$ with the coordinate $\mathbf{r}$. The electron's wavefunction $u(\mathbf{R},\mathbf{r})$ and the energy $E(\mathbf{R}$ both depend on the position of the nuclei $\mathbf{R}$ as a parameter. The last step in Born-Oppenheimer approximation is to solve the Schrodinger equation for the nuclei, using the above calculated $E(\mathbf{R})$ as a potential energy, which leads to a following equation.

$$\left[-\frac{1}{2}\nabla_R^2 + E(\mathbf{R})\right] v(\mathbf{R}) = \epsilon v(\mathbf{R}) \tag{2.15}$$

Once these operations are carried, the Born-Oppenheimer approximation states that the energy ϵ is a good approximation of the energy levels of the exact Schrodinger equation (2.2) As a result, the total molecular wave function is separated into the electronic and the nuclear wavefunction.

$$\psi(\mathbf{R}, \mathbf{r}) = u(\mathbf{R}; \mathbf{r})v(\mathbf{R}) \tag{2.16}$$

In addition, each electronic eigenvalue $E_n(R)$ will give a rise to the electronic surface, known as Born-Oppenheimer surfaces. Therefore the full internuclear potential will be given as $V_{NN}(R) + E_n(R)$.

One could proceed further for the complete treatment of the Born-Oppenheimer approximation, for example dealing with the Born-Oppenheimer diagonal correction[?] , but it will go beyond the scope of this thesis .

At this moment, using BO approximation we have a Schrodinger equation for the electron, orbiting the two nuclei (each consisting of a single proton). Note that in the further text the ψ will denote the function $u(\mathbf{R}; \mathbf{r})$, since it is customary to denote the wave function as ψ.

2.2 Replicating the 3D Solution for the H_2^+ Molecular Ion

2.2.1 Solution Process

Following the seminal papers by Bates et. all.[? ?] , we can re-express the equation as:

$$\left(-\frac{1}{2}\nabla^2 - \frac{1}{r_a} - \frac{1}{r_b}\right)\psi = E\,\psi \tag{2.17}$$

where $r_a = \left|\mathbf{r} - \frac{1}{2}\mathbf{R}\right|$ and $r_b = \left|\mathbf{r} + \frac{1}{2}\mathbf{R}\right|$ are distances of the electron from the nuclei and $\mathbf{R}$ is a distance between nuclei.

Due to the cylindrical symmetry of the problem, we choose the elliptical coordinates. We follow[?] , where authors chose the confocal elliptic co-ordinates $\lambda,\ \mu$, which transforms the coordinates r_a and r_b from (2.17) into:

$$r_a = \frac{R}{2}(\lambda + \mu)\,, \quad r_a = \frac{R}{2}(\lambda - \mu) \tag{2.18}$$

After applying the coordinate transformations (2.18) into the equation (2.17), we obtain another partial differential equations[?] :

$$\frac{d}{d\lambda}\left\{(\lambda^2-1)\frac{d\psi}{d\lambda}\right\}+\frac{d}{d\mu}\left\{(1-\mu^2)\frac{d\psi}{d\mu}\right\}+\left\{\frac{1}{\lambda^2-1}+\frac{1}{1-\mu^2}\right\}\frac{d^2\psi}{d\phi^2}+\left\{\frac{1}{4}R^2E(\lambda^2-\mu^2)+2R\lambda\right\}\psi=0 \tag{2.19}$$

We assume that the solution can be separated, in the product of the two functions of the single variable, λ, μ, ϕ. Under this assumption the solution can written as:

$$\psi(\lambda,\mu,\phi) = L(\lambda)M(\mu)e^{im\phi} \quad \text{where is} \quad p^2 = -\frac{1}{4}R^2E \tag{2.20}$$

In this equation the L, M are the functions of their respective coordinates, and m is an integer, either positive or negative. The next step is to insert the ansatz (2.20) into the Eq (2.19) . After some algebra, one observes that the equation (2.19) separates into the system of two ordinary, coupled differential

equations. an

$$\frac{d}{d\mu}\left\{(1-\mu^2)\frac{dM}{d\mu}\right\}+\left\{-A+p^2\mu^2-\frac{m^2}{1-\mu^2}\right\}M=0 \tag{2.21}$$

$$\frac{d}{d\lambda}\left\{(\lambda^2-1)\frac{dL}{d\lambda}\right\}+\left\{A+2R\lambda-p^2\lambda^2-\frac{m^2}{\lambda^2-1}\right\}L=0 \tag{2.22}$$

In[?] , Bates et al. state that they used the method of successive approximation to found the coefficients in the series. It was tacitly assumed that the successive approximation themselves converge. The approximation is terminated either when the desired precision is achieved of when the certain number of approximation is met. However the details of the numerical calculation are not provided in the paper.

2.2.2 Differential Operator Spectrum

We can view the equations for M and L as the eigenvalue operator equations $D^1\,M(\mu)=A\,M(\mu)$ and $D^2\,L(\lambda)=-A\,L(\lambda)$. Since these equations model a real, physically realizable system, we assume that operators $D^{1,2}$ are compact on l^2 space, therefore each $D^{1,2}$ operator satisfies:

$$\|D_n^{1,2}\rightarrow D^{1,2}\| \tag{2.23}$$

where $D_n^{1,2}=P_nD^{1,2}P_n$ So with these assumptions, operators $D^{1,2}$ can be approximated by the finite dimensional matrices.

2.2.3 TOWARDS THE SOLUTION

Here we replicate the solution of Bates et. all.[? ?] , by using a more of a brute force approach. The idea is to numerically calculate the spectrum of a differential operator to a desired precision We expressed equations (2.21),(2.22) as a matrix eigenvalue problem. The system (2.21),(2.22) of the two ODEs then depend on the two parameters, total energy E, and the separation constant A. The problem is reduced to finding those values of E and A for which the solution to the differential equation satisfy the requisite boundary conditions. Since it is a Sturm-Liouville problem, or more precisely a system of two Sturm-Liouville problems, our approach is fundamentally the same approach as taken by Bates. but it is more practical, as it can better accommodate the existing numerical software. There exist excellent numerical packages[?] for computing the matrix eigenvalues, and they greatly simplify the actual computation.

We express both function $M(\mu)$ and $L(\lambda)$ using the set of orthogonal functions which satisfy the boundary conditions. We then follow the method of Frobenius. Once we replace the assumed solution into the equation and after some algebra, we obtain effectively two uncoupled, infinite systems of equations, where the unknowns are the coefficients in the solution series. The solution vector depends on the two parameters, p, which is the function of energy and A which is the separation constant.

The next step is rather simple. For functions $M(\mu)$ and $L(\lambda)$, we need to find

the functional dependency of the parameters p and A, so that solution exists. The intersections of the two curves $p_1 = f(A_1)$ and $p_2 = g(A_2)$ provides the value of p and A when the condition for the solutions exists. The desired precision is obtained by choosing the size number of terms in the series.

The remaining issue is that even with the modern fast computers and optimized numerical libraries[?] , calculating eigenvalues is a slow process. The complexity of the QR decomposition algorithms is $O(n^3)$[?] , which make the QR factorization feasible by today's computer systems, but fairly slow for large matrices.

2.3 Series Expansions and Eigenvalue Determinant

Here we describe in details the method describe in the previous section.

2.3.1 L Equation

Start with:

$$\begin{aligned} &\frac{d}{d\lambda}\left\{\left(\lambda^2-1\right)\frac{d\Lambda}{d\lambda}\right\}+\left\{A-p^2\lambda^2+2R\lambda\right\}\Lambda=0\Rightarrow \\ &\left(\lambda^2-1\right)\frac{d^2\Lambda}{d\lambda^2}+2\lambda\frac{d\Lambda}{d\lambda}+\left\{A-p^2\lambda^2+2R\lambda\right\}\Lambda=0 \end{aligned} \tag{2.24}$$

For practical reasons we first shift the L equation b $x=\lambda-1$ to obtain:

$$\frac{d}{d\,x}\left\{x(x+2)\frac{d\,\Lambda}{d\,x}\right\}+\left\{-p^2\,x^2+(-2p^2+2R)x-p^2+2R+A\right\}\Lambda=0$$

$$x(x+2)\frac{d^2\,\Lambda}{d\,x^2}+(2x+2)\frac{d\,\Lambda}{d\,x}+\left\{-p^2\,x^2+(-2p^2+2R)x-p^2+2R+A\right\}\Lambda=0 \tag{2.25}$$

Now we assume that the solution exists and that it can be represented as the sum of Laguerre polynomials:

$$\Lambda(x)=e^{-px}\sum_{n=0}^{\infty}c_n\,L_n(x) \tag{2.26}$$

Inserting the ansatz (2.26) into (2.25), applying the properties of Laguerre's polynomial some algebra we obtain.

$$\begin{aligned}
&-2p\sum_{n=0}^{\infty}c_n\,n(2n+1)L_n+2p\sum_{n=0}^{\infty}c_{n+1}\,n(n+1)L_{n+1}+2p\sum_{n=0}^{\infty}c_{n-1}\,n^2L_{n-1}+\\
&+(2p-1)\sum_{n=0}^{\infty}c_{n-1}n(2n-1)L_{n-1}-(2p-1)\sum_{n=0}^{\infty}c_nn^2L_n-\\
&-(2p-1)\sum_{n=0}^{\infty}c_{n-2}n(n-1)L_{n-2}+(-2p+2R)\sum_{n=0}^{\infty}c_n(2n+1)L_n-\\
&-(-2p+2R)\sum_{n=0}^{\infty}c_{n+1}(n+1)L_{n+1}-(-2p+2R)\sum_{n=0}^{\infty}c_{n-1}nL_{n-1}+\\
&+(-4p+1)\sum_{n=0}^{\infty}c_n\,n\,L_n+(4p+1)\sum_{n=0}^{\infty}c_{n-1}\,n\,L_{n-1}+\\
&+(-2p-p^2+2R+A)\sum_{n=0}^{\infty}c_n\,L_n=0
\end{aligned} \tag{2.27}$$

The next step is to multiply the equation (2.27) with $e^{-x}L_m(x)$ and integrate

from 0 to ∞ using the orthogonality property of the Laguerre's polynomials: $\int_0^\infty dx\, e^{-x} L_n(x) L_m(x) \;=\; \delta_{mn}$ to obtain the recurrence equations for the unknown coefficients c_n

$$
\begin{aligned}
&-2p\,n(2n+1)c_n + 2p\,n(n+1)c_{n+1} + 2p\,n^2 c_{n-1} + (2p-1)n(2n-1)c_{n-1} - \\
&-(2p-1)n^2 c_n - (2p-1)n(n-1)c_{n-2} + (-2p+2R)(2n+1)c_n - \\
&-(-2p+2R)(n+1)c_{n+1} - (-2p+2R)nc_{n-1} + (-4p+1)\,n\,c_n + \\
&+(4p+1)\,n\,c_{n-1} + (-2p-p^2+2R+A), c_n = 0
\end{aligned}
\tag{2.28}
$$

This expression (2.28) is a system of linear equations, where the unknowns are the coefficients c_n. The coefficients multiplying the unknowns c_n in (2.28) form the band matrix.

2.3.2 M EQUATION

We the same approach for the M equation.

$$
\frac{d}{d\,\mu}\left\{\left(1-\mu^2\right)\frac{d\,M}{d\,\mu}\right\} + \left(-A + p^2\mu^2\right) M(\mu) = 0 \tag{2.29}
$$

We express the $M(\mu)$ as the series of Legendre polynomials.

$$
M(\mu) = \sum_{n=0}^{\infty} f_n\, P_n(\mu) \tag{2.30}
$$

where

$$\int_{-1}^{1} P_m(x)P_n(x)dx = \frac{2}{2m+1}\delta_{m,n} \tag{2.31}$$

Substituting (2.30) into (2.29), multiplying by $P_m(\mu)$, and integrating from -1 to 1 we obtain

$$\sum_{n=0}^{\infty}\Big\{-\int_1^1 P_m(\mu)n(n+1)P_n(\mu)d\mu - A\int_1^1 P_m(\mu)P_n(\mu)d\mu +$$

$$+\,p^2\int_1^1 P_m(\mu)\mu^2 P_n(\mu)d\mu\Big\} = 0 \quad \text{or} \tag{2.32}$$

$$\sum_{n=0}^{\infty}\left\{\frac{-2}{2n+1}n(n+1)\delta_{m,n} - A\frac{2}{2n+1}\delta_{m,n} + p^2\int_1^1 P_m(\mu)\mu^2 P_n(\mu)d\mu\right\} = 0$$

Taking advantage of the orthogonality of Legendre Polynomials (2.31), we obtain a system of linear equations, where the coefficients form a band matrix.

$$\sum_{n=0}^{\infty}\left\{\frac{-2n(n+1)}{2n+1}\delta_{m,n} - A\frac{2}{2n+1}\delta_{m,n} +\right.$$

$$+p^2\frac{2}{2n+1}\left[\frac{(n+1)^2}{(2n+1)(2n+3)} + \frac{n^2}{(2n+1)(2n-1)}\right]\delta_{m,n} +$$

$$\left.p^2\frac{2(n+1)(n+2)}{(2n+1)(2n+3)(2n+5)}\delta_{m,n+2} + p^2\frac{2\,n(n-1)}{(2n+1)(2n-1)(2n-3)}\delta_{m,n-2}\right\} = 0 \tag{2.33}$$

In appendix B we present the Mathematica code for calculating electron energies of the molecular H^2 ion in 3 dimensions using Mathematica eigenvalue solver.

2.3.3 NUMERICAL CALCULATION

Equations (2.28) and (2.33) constitute the couple system of linear equation. Each series is parameterized by 2 parameters, p and A , as well as the parameter R, the distance between nuclei. We select the values of R as shown in table **??**. We tacitly assume that the series (2.26) (2.29) converge, moreover, we assume that they converge uniformly. Therefore, we truncate the series at some index $i = K$, chosen to achieve the desired accuracy. Now the coefficient matrices are dimensions $K \times K$ and each matrix has K eigenvalues, and the lowest eigenvalue corresponds to the lowest value of p, thus to the lowest energy.

In next step, for each value of R, we calculate the eigenvalues, sort them, and pick the lowest (or the i-th one from the bottom), and view them as functions $A = A(p)$. So for each of the equations (2.28) and (2.33), we choose the interval $[0, 2 * R]$ and divide it into N points $p_i, i = 1..N$. For each point, we calculate, sort and pick desired the eigenvalue of the matrix M (L). That way we obtain two functions $A_M = A_M(p)$ and $A_L = A_L(p)$, evaluated at points p_i. We interpolate these two functions, using Wolfram's Mathematica 3-rd order Spline interpolation. As a side note, for a small subset of values R we used the higher order Spline interpolation but we were unable to observe the difference in the results obtained. The intersection of these two curves in the value of p for which both $M(\mu)$ and $L(\lambda)$ equations have results satisfying the boundary conditions. Now we repeat the calculation for the next value of

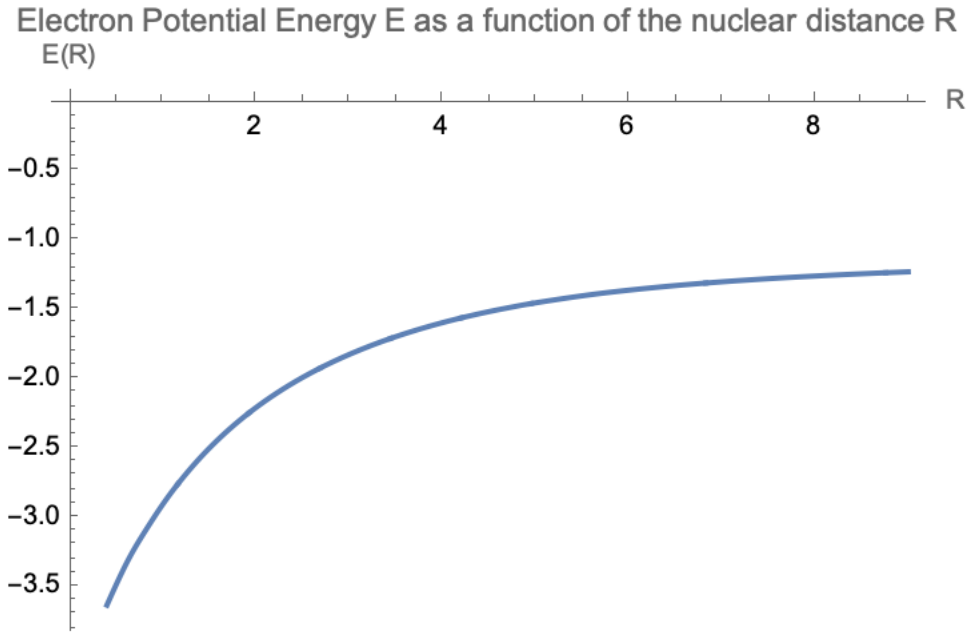

R.

After all this exercise, we get the function $E = E(R)$, from (2.14) which is the electron energy in the BO approximation. Adding the potential energy between nuclei is $V(R) = 1/R$, we obtain the potential energy curve. The paper by Bates does not explicitly use this curve to calculate the vibrational energies, but we will, in our 2D case.

For illustration purposes we present some of the results below.

Plot of the ground state energies $E(R)$ and $E(R) + V(R)$ where $V(R) = \frac{1}{R}$ represents the potential energy of the nuclei.

Electron energy as an eigenvalue of the equations (2.28) and (2.33).

Total energy, calculated by adding the potential energy of the nuclei $V(R) =$

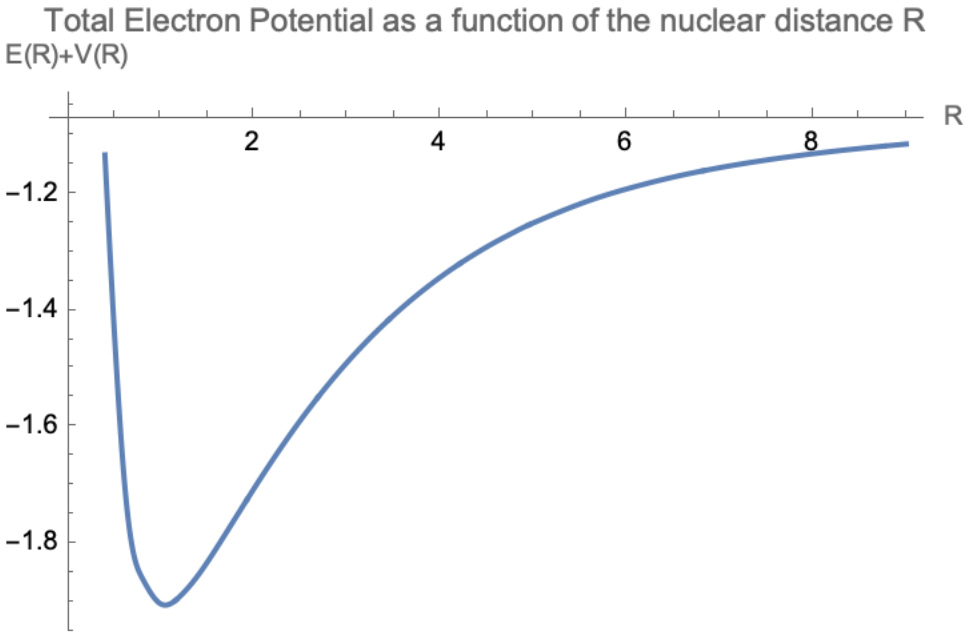

$1/R$.

Electron energy as an eigenvalue of the equations (2.28) and (2.33).

Table comparing the electron energies obtain using our method vs method applied by Bates et al. We chose a subset of values to indicate the overall trend.

Table 2.1: Electron Energy, $1s\sigma_g$ state

R	-E(R) (Bates)	-E(R) (our method)
0.4	3.60157	3.632200
0.6	3.34301	3.3429676
0.8	3.10895	3.1089586
1.0	2.90356	2.9035720
1.2	2.72461	2.7246154
1.4	2.56853	2.5685373
1.6	2.43186	2.4318740
1.8	2.31162	2.3116176
2.0	2.20525	2.2052681
2.2	2.11076	2.1107695
2.4	2.02642	2.0264405
2.6	1.95090	1.9508966
2.8	1.88299	1.8829977
3.0	1.82178	1.8217919
3.2	1.76647	1.7664850
3.4	1.71639	1.7164029
3.6	1.67097	1.6709739
3.8	1.62971	1.6297050
4.0	1.59216	1.5921695
4.2	1.55799	1.5579948
4.4	1.52685	1.5268516
4.6	1.49844	1.4984480
4.8	1.47252	1.472523
5.0	1.44884	1.448840

CHAPTER 3

NON-RELATIVISTIC SOLUTION OF THE HYDROGEN MOLECULAR ION IN 2 SPATIAL DIMENSIONS

3.1 EXISTING SOLUTIONS

We apply similar method used in the 3D case of the H_2^+ ion to find the solution in 2 dimensions. The problem itself is analogous to the 3D problem, but leads to the Mathieu's function as the solution for the radial problem.

There are not too many papers dealing with solving the H_2^+ but here is some relevant, and recent work in this problem. In addition to the Bates paper[?], there are other, more recent papers[? ?,?] which deal with the solution of the Schrodinger equation and spectrum of the H_2^+ molecule. As with other work in this problem, the paper relies on the work done by Bates et all.[?]. The solution in[?] agrees well with our solution. One can also apply approximate methods, but they should be considered inferior to the analytical solution, we provide here.

Analogous to the 3D case, we rely on Born-Oppenheimer (BO) approximation, in order to provide an analytical solution. The same justification for using the BO approximation in 3D molecular systems applies to the 2D problems as well, since the masses of the nuclei and electron(s) remain unchanged. Following the same BO approximation as in Chapter 1, and using atomic units, the Schrodinger equation for the H_2^+ molecules is given by equation (3.1) below.

$$\left(-\frac{1}{2}\nabla^2 - \frac{1}{r_a} - \frac{1}{r_b}\right)\psi = E\,\psi \tag{3.1}$$

The equation (3.1) is superficially similar to the equation (2.17) and the diagram 2.1, but in this case, the r_a and r_b represent the nuclei coordinates in 2 dimensions.

Following the[?] , The electron wavefunction depends on only 3 quantum numbers, principal quantum number n, angular quantum number l and spin s. Again we ignore the spin degrees of freedom, considering the electron to be the regular 3 dimensional particles, where only its orbit is restricted to 2 dimensions. Therefore the spin magnetic moment of the electron is not affected by the 2D restriction and the spin vector can point in any direction in 3D space. Also the orbit can have different shapes, thus there remains the need for an orbital quantum number. However, there can be one one orientation of the orbit, thus we do not consider the magnetic quantum number. This reasoning agrees with the solution of the electron wavefunction to the hydrogen

atom in 2 dimensions[?] where electron wavefunction solution only depends on the principal and orbital quantum numbers.

The geometry of the 2D problem leads to choosing the elliptical coordinates (as in 3D problem), with two coordinates, μ and λ denoting the position of the electron in 2D plane.[?]

3.2 EXACT SOLUTION OF THE ELECTRON ENERGIES OF THE H_2^+ MOLECULE

The goal is to provide the exact solution to the wavefunction of the H_2^+ electron, for a given definition of exact. However even for this, relatively simple problem, it is impossible to find a closed form solution. So the solution is exact, in the sense that it can be done to an arbitrary precision.

As illustrated by the figure 3.1, we express equation (3.1) in the elliptical coordinates, and by setting the x axis to be perpendicular to the internuclear axis, we have the nuclei at: $y = \pm\frac{R}{2}$, R being the distance between nuclei. So in 2D elliptic coordinates, λ, μ we have:

$$\lambda = (r_a + r_b)/R; \qquad \mu = (r_a - r_b)/R$$

where $\lambda \in [1, \infty]$, $\mu \in [-1, 1]$ and (3.2)

$$r_a = \frac{R}{2}(\lambda + \mu) \qquad r_b = \frac{R}{2}(\lambda - \mu)$$

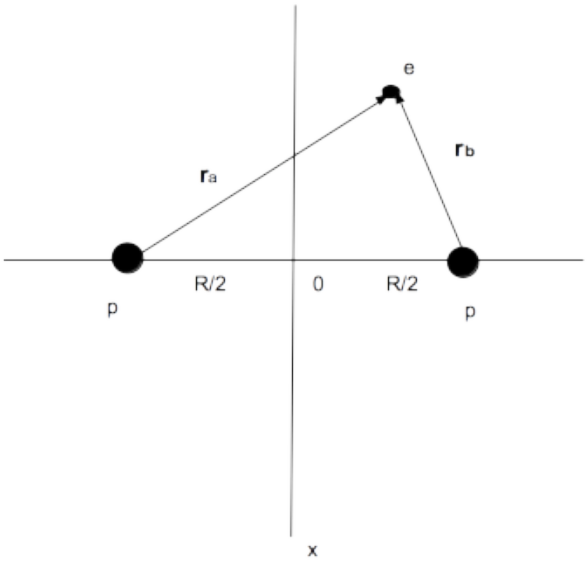

Figure 3.1: Hydrogen Ion in 2 dimension

We assume that the total electronic wavefunction can be written as the product of two functions:

$$\psi(\lambda, \mu) = F(\mu)G(\lambda) \tag{3.3}$$

This way the original equation separates into two ODEs:

$$\left(\lambda^2 - 1\right) \frac{d^2}{d\lambda^2} G(\lambda) + \lambda \frac{d}{d\lambda} G(\lambda) + \left(A + \frac{E\,R^2}{2}\lambda^2 + 2R\lambda\right) G(\lambda) = 0 \tag{3.4}$$

$$\left(1-\mu^2\right)\frac{d^2}{d\mu^2}F(\mu)-\mu\frac{d}{d\mu}F(\mu)+\left(-A-\frac{E\,R^2}{2}\mu^2\right)F(\mu)=0 \tag{3.5}$$

and A is the separation constant. At this point we set:

$$p^2=-\frac{ER^2}{2} \tag{3.6}$$

The rest of the derivation is in the appendix C.

3.2.1 M EQUATION

Following the derivation in appendix C we get for the M equation

$$\frac{d^2M}{dx^2}+\left[-A+\frac{p^2}{2}+\frac{p^2}{2}\cos(2x)\right]M=0 \tag{3.7}$$

The equation (3.7) is a form of a Mathieu's equation[?] .

3.2.2 L EQUATION

Following the derivation in appendix C we get for the L equation

$$(\lambda^2-1)\frac{d^2\,L}{d\lambda^2}+(2k+1)\lambda\frac{d\,L}{d\lambda}+\left[A+\frac{E\,R^2}{2}\lambda^2+2R\lambda-k\right]L(\lambda)=0 \tag{3.8}$$

The equation for the $L(\lambda)$ looks similar to the radial (modified) Mathieu's equation, but it is not an exact identity.

We observe that both equations for the functions $M(\mu)$ and $L(\lambda)$ are either

exact match or related to the Mathieu's equations. In general the Mathieu's equation represents the standing wave on an elliptical drum, (2D space), and the solution for the time independent Schrodinger equation is in general a standing wave, in 2D in this case. So it is plausible that these types of solutions are similar.

ALGEBRAIC SOLUTION

The equation $(??)$ can be written as:

$$\frac{d^2M}{dx^2} + [w - 2q\cos(2x)]\,M = 0 \tag{3.9}$$

where

$$\begin{aligned} w &= -A + \frac{p^2}{2} \\ q &= -\frac{p^2}{2} \end{aligned} \tag{3.10}$$

From the geometry of the problem we conclude that $M(\mu)$ must be an even function. Following[?] we look for the solution as class I and class II, which has even and odd eigenvalue functions as:

$$V_0 = \cfrac{2}{V_2 - \cfrac{1}{V_4 - \cfrac{1}{V_6 - ...}}} \tag{3.11}$$

$$V_1 - 1 = \cfrac{1}{V_3 - \cfrac{1}{V_5 - \cfrac{1}{V_7 - ...}}} \tag{3.12}$$

where

$$V_m = \frac{w - m^2}{q} \tag{3.13}$$

The equations 3.11 and 3.12 provide the first gen equation for the even and odd solution respectively.

There are actually two ways to try to solve this equation:

Following[?] and[?] we look for the solution in the form of:

$$L(\lambda) = (\lambda + 1)^{\sigma} e^{-p\lambda} \sum_{n=0}^{\infty} a_n x^n \tag{3.14}$$

with

$$\sigma = \frac{R}{p} - \frac{1}{2} \quad \text{and} \quad x = \frac{\lambda - 1}{\lambda + 1} \tag{3.15}$$

Substituting (3.14) into $(\mathrm{C}.9)$ and after some formidable algebra, we get a recurrence relation:

$$\alpha_n a_{n+1} - \beta_n a_n + \gamma_n a_{n-1} = 0 \quad n \geq 0 \tag{3.16}$$

with

$$\alpha_n = (n+1)\left(n+\frac{1}{2}\right)$$

$$\beta_n = \left[2n^2 + (4p-2\sigma)n - A + p^2 - 2p\sigma - \frac{\sigma}{2}\right] \tag{3.17}$$

$$\gamma_n = (n-1)\left(n-2\sigma-\frac{1}{2}\right) + \sigma\left(\sigma-\frac{1}{2}\right)$$

and if follows that

$$\frac{a_n}{a_{n-1}} = F_n \quad \text{where} \quad F_n = \cfrac{\gamma_n}{\beta_n - \cfrac{\alpha_n\gamma_{n+1}}{\beta_{n+1} - \cfrac{\alpha_{n+1}\gamma_{n+1}}{\beta_{n+1} - \ldots}}} \tag{3.18}$$

Since $a_{-1} = 0$ we have

$$\frac{\beta_0}{\alpha_0} = F_1 \tag{3.19}$$

The Mathematica code is in appendix D. The energies calculated and the plot of the potential for the states $1s_g^+$ and $2s_g^+$ are in the tables below.

LAGUERRE POLYNOMIALS AND THE OPERATOR SPECTRUM

Here we use a more of a brute force approach. We keep the equation for μ since it is a Mathieu's equation, with a well known solutions. For the λ equation, we numerically calculate the spectrum of a differential operator to a desired precision

For the equation (3.8) one could proceed by following the radial Mathieu's equations approach. One way to solve the Radial Mathieu's equation is by

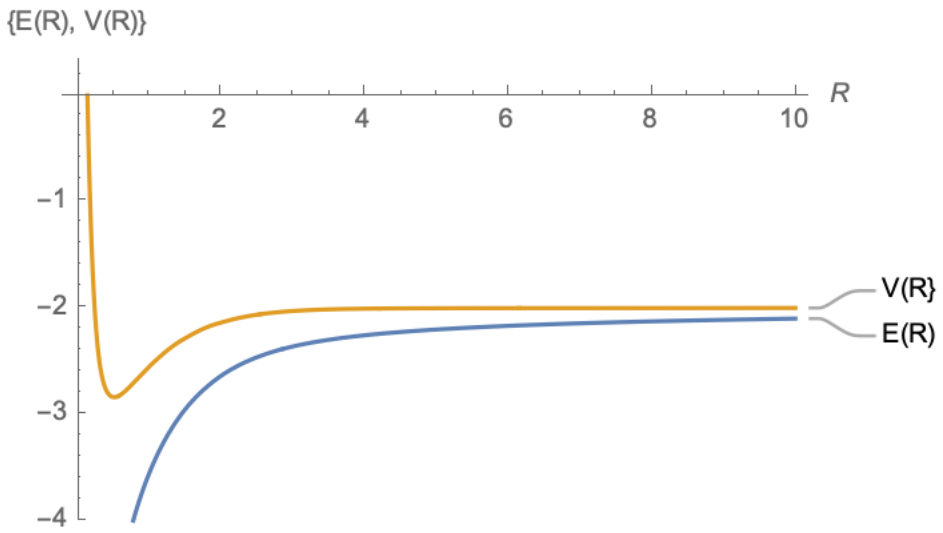

Figure 3.2: H_2^+ Energy and Potential curves for the $1s_g^+$ state

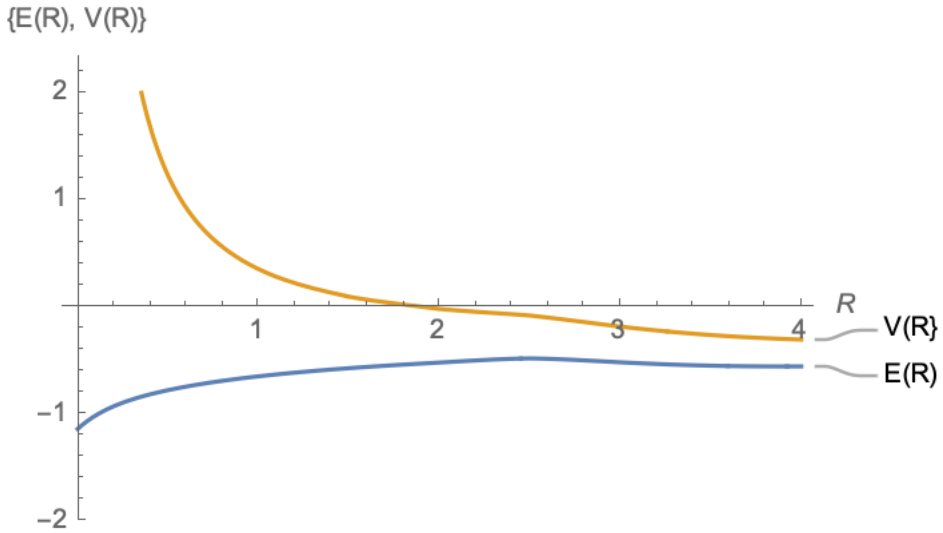

Figure 3.3: H_2^+ Energy and Potential curves for the $2s_g^+$ state

Table 3.1: The separation constant A, electronic energy E

total energy $E + \frac{1}{R}$, for the state $1s_g$ some values of the internuclear separation R

R	p	A	E	$E + \frac{1}{R}$
0.1	0.1915	7.2704	-7.3359	2.6640
0.2	0.3606	7.3367	-6.5033	-1.5033
0.3	0.5117	7.4029	-5.8197	-2.4864
0.4	0.6496	7.4684	-5.2754	-2.7754
0.5	0.7776	7.5332	-4.8382	-2.8382
0.6	0.8981	7.5974	-4.4814	-2.8148
0.7	1.0127	7.6608	-4.1861	-2.7575
0.8	1.1226	7.7235	-3.9385	-2.6885
0.9	1.2288	7.7856	-3.7286	-2.6174
1.0	1.3321	7.8469	-3.5490	-2.5490
1.5	1.8219	8.1444	-2.9508	-2.2841
2.0	2.2962	8.4273	-2.6363	-2.1363
2.5	2.7738	8.6973	-2.4620	-2.0620
3.0	3.2594	8.9556	-2.3608	-2.0275
3.5	3.7516	10.6100	-2.2979	-2.0122
4.0	4.2479	14.0730	-2.2556	-2.0056
4.5	4.7464	18.0513	-2.2250	-2.0028
5.0	5.2459	22.5391	-2.2015	-2.0015
6.0	6.2459	33.0272	-2.1673	-2.0006
7.0	7.2462	45.5209	-2.1431	-2.0003
8.0	8.2463	60.0130	-2.1250	-2.0000
9.0	9.2458	76.4955	-2.1107	-1.9996
10.0	10.2444	94.9542	-2.0989	-1.9989

using the series of hyperbolic functions, obtained from the solution of angular Mathieu's equation using the substitution $\eta = i\,\xi$. But that this approach in numerically unstable and hard to compute? . There is another approach, using the product of Bessel Functions?

We took a different approach to solving the equation (3.8), namely look for the

Table 3.2: The separation constant A, electronic energy E

total energy $E + \frac{1}{R}$, for the state $2s_g$ for some values of the internuclear separation R

R	p	A	E	$E + \frac{1}{R}$
0.1	0.0710	15.8560	-1.0102	8.9897
0.2	0.1358	19.2757	-0.9225	4.0770
0.3	0.1967	22.4772	-0.8600	2.4730
0.4	0.2548	25.4103	-0.8116	1.6883
0.5	0.3106	28.1052	-0.7722	1.2277
0.6	0.3647	30.6031	-0.7390	0.9275
0.7	0.4172	32.9399	-0.7105	0.7179
0.8	0.4684	35.1437	-0.6856	0.5643
0.9	0.5183	4.9531	-0.6634	0.4476
1.0	0.5672	5.1105	-0.6436	0.3563
1.5	0.7991	48.1936	-0.5676	0.0989
2.0	1.0152	6.6787	-0.5153	-0.0153
2.5	1.2202	7.4617	-0.4765	-0.0765
3.0	1.5192	8.2456	-0.5129	-0.1795
3.5	1.8256	10.6103	-0.5441	-0.2584
4.0	2.0993	14.0727	-0.5509	-0.3009
4.5	2.3464	18.0503	-0.5437	-0.3215
5.0	2.5728	22.5360	-0.5295	-0.3295
6.0	2.9809	33.0090	-0.4936	-0.3269
7.0	3.3483	45.4488	-0.4575	-0.3147
8.0	3.6890	59.7980	-0.4252	-0.3002
9.0	4.0122	75.9727	-0.3974	-0.2863
10.0	4.3243	93.8641	-0.3739	-0.2739

solution in the form of the series of orthogonal functions. This approach has some challenges, since on a finite interval, there are number of functions orthogonal the interval, and one can choose the one which fits the problem the best. On an infinite interval, such as $\lambda = [1, \infty]$ the choice is somewhat limited. The Laguerre's polynomial seemed like a suitable choice, as they form an orthogonal set on the infinite interval. So we look for the solution in the

form:

The power series method is described in numerous textbooks are papers. It is tacitly assumed that the solution to the differential equation is a 'well behaved' continuous function and that consequently the power series converges.

So assume the solution as the sum of Laguerre polynomials:

$$L(\lambda) = e^{-p\lambda} \sum_{k=0}^{\infty} c_k \, L_k(\lambda) \tag{3.20}$$

Where $L_n(\lambda)$ are Laguerre polynomials. They have several interesting properties, which can be found in[?] .

We insert the equation 3.20 into 3.8, expand, cancel and collect.

The detailed derivation is described in appendix C.

Now multiply by $L_m(x)$ and use the orthogonality of Laguerre's polynomials to obtain the n x n matrix with the parameter p which has eigenvalues A.

So using the solutions above, the next step is to find the eigenvalues A, p, of the equations $(\mathbf{??})$ and (3.8). Using the series above, for each equation, we find functions $A_i(p)$ for which the solution exists. The intersection of the two functions $A_i(p)$ is the value of p common for both equations (3.7) and (3.8). This procedure translates into the matrix eigenvalues problem, following the steps below.

The detailed derivation is in appendix C.

The rest of the work is numerical. Since our goal is to obtain the function $E(R)$

we choose the suitable values of R as in table **??** . For each value of R we divide with the interval $p \in [0, 2 * R]$ into the n points. For each value of p we calculate store the eigenvalues for equation for $M(\mu)$ and $L(\lambda)$. Finding matrix eigenvalues is a common operation is a number of fields, and good numerical algorithms and libraries are available, such as[?] .

I have used Wolfram Mathematica, to all numerical work. It is easier to use and obtain results, as well as process them in tables and graphs. ‘

The results of the brute force approach are in the table below. When compared to the algebraic results above, the brute force results are less accurate, and much worse for the small values or R. It is probably due to the numerical instability of the eigenvalue equation. Also the infinite series solution in the algebraic method is more ’precise’ than the general solution series in the brute force method.

So in the subsequent chapters, we shall use the results from the algebraic approach.

Table 3.3: The separation constant A, electronic energy E

total energy $E + \frac{1}{R}$, for the state $1s_g$ for some values of the internuclear separation R

R	p	A	E	$E + \frac{1}{R}$
0.2	0.2031	0.0206	-2.0636	2.9363
0.3	0.2874	0.0415	-1.8358	1.4975
0.4	0.6483	0.2156	-5.2538	-2.7538
0.5	0.7763	0.3126	-4.8216	-2.8216
0.6	0.8968	0.4223	-4.4686	-2.8019
0.7	1.0115	0.5440	-4.1760	-2.7474
0.8	1.1214	0.6777	-3.9304	-2.6804
0.9	1.2277	0.8236	-3.7220	-2.6109
1.0	1.3311	0.9820	-3.5436	-2.5436
1.5	1.7848	1.8037	-2.8318	-2.1651
2.0	1.9182	1.3252	-1.8398	-1.3398
2.5	1.9383	0.2865	-1.2022	-0.8022
3.0	1.9588	-0.7551	-0.8526	-0.5193
3.5	2.1000	-2.2367	-0.7200	-0.4342
4.0	2.1121	-2.2039	-0.5576	-0.3076
4.5	2.3541	-1.8836	-0.5473	-0.3251
5.0	2.5797	-1.5553	-0.5323	-0.3323
6.0	2.9869	-0.9144	-0.4956	-0.3290
7.0	3.3539	-0.2604	-0.4591	-0.3162
8.0	3.6945	0.4400	-0.4265	-0.3015
9.0	4.0177	1.2162	-0.3985	-0.2874
10.0	10.6696	78.8425	-2.2768	-2.1768

Table 3.4: The separation constant A, electronic energy E

total energy $E + \frac{1}{R}$, for the state s_g some values of the internuclear separation R

R	p	A	E	$E + \frac{1}{R}$
0.2	0.1988	0.0198	-1.9764	3.0235
0.3	0.3290	0.0545	-2.4061	0.9272
0.4	0.3284	0.0543	-1.3484	1.1515
0.5	0.2995	0.0451	-0.7179	1.2820
0.6	0.2801	0.0394	-0.4360	1.2306
0.7	0.4074	0.0838	-0.6774	0.7510
0.8	0.4583	0.1063	-0.6563	0.5936
0.9	0.5080	0.1311	-0.6374	0.4736
1.0	0.5574	0.1583	-0.6214	0.3785
1.1	0.6047	0.1870	-0.6045	0.3044
1.5	0.7887	0.3230	-0.5529	0.1137
2.0	1.0048	0.5365	-0.5048	-0.0040
2.5	1.2100	0.7982	-0.4685	-0.0680
3.0	1.4072	1.1096	-0.4400	-0.1067
3.5	1.5984	1.4732	-0.4171	-0.1314
4.0	1.7690	1.7037	-0.3911	-0.1411
4.5	1.9109	1.6840	-0.3606	-0.1384
5.0	1.9374	0.3310	-0.3003	-0.1003
6.0	1.9970	-2.2878	-0.2215	-0.0549
7.0	2.2709	-2.0010	-0.2105	-0.0676
8.0	2.5364	-1.6194	-0.2010	-0.0760
9.0	2.7887	-1.2354	-0.1920	-0.0809
10.0	11.3799	108.2679	-2.5900	-2.4900

CHAPTER 4

2D SCATTERING

Here we briefly address the scatering in 2 dimensions.

The quantum scattering in 3 dimension is described in numerous textbooks and papers, so we ommit explicitly referencing them here.

Scattering in 2 dimensions follows the same approach as in 3D, with some subtle differences. We start with the Schrodinger equation in 2 dimensions:

$$\left(-\frac{1}{2}\nabla^2 + V(\mathbf{r})\right)\psi(\mathbf{r}) = E\psi(\mathbf{r}) \tag{4.1}$$

In polar coordinates:

$$\left[-\frac{\partial^2}{\partial r^2} - \frac{1}{r}\frac{\partial}{\partial r} - \frac{1}{r^2}\frac{\partial^2}{\partial \phi^2} + V(r)\right]\psi(r,\phi) = 2E\ \psi(r,\phi) \tag{4.2}$$

Using separation of variables: $\psi(r,\phi) = F(r)T(\phi)$, we end up with 2 ordinary

differential equations. We set $-k^2 = 2E$

$$\begin{aligned} &\frac{d^2F(r)}{dr^2} - \frac{1}{r}\frac{dF(r)}{dr} + (k^2 - 2V(r) - \frac{m^2}{r^2})F(r) = 0 \\ &\frac{d^2T(\phi)}{d\phi^2} + m^2T(\phi) = 0 \end{aligned} \tag{4.3}$$

The function $T(\phi)$ must be single valued and symmetric around the incident beam, taken to be around x. In that case, m must be an integer, and normalized angular function is:

$$T(\phi) = \frac{1}{\sqrt{\pi 2}} \cos m\phi \tag{4.4}$$

where m is an integer.

The radial equation $F(r)$ is:

$$\frac{d^2F}{dr^2} + \frac{1}{r}\frac{dF}{dr} + \left(k^2 - 2V(r) - \frac{m^2}{r^2}\right) F = 0 \tag{4.5}$$

By examining the domain of the equation (4.5), we can identify 2 regions:

FAR AWAY REGION

For the regions far away from the scattering area where $V(r) \to 0$ we have a free space Schrodinger equation with $k^2 = -E$;

$$\frac{d^2F(r)}{dr^2} + \frac{1}{r}\frac{dFr(r)}{dr} + \left(k^2 - \frac{m^2}{r^2}\right) F(r) = 0 \tag{4.6}$$

This is a second order wave equation whose general solution looks like the combination of the incoming and outgoing wave, i.e. $\psi(r) = R(r)e^{\pm ikr}$.

Following[?] we are interested in outgoing wave only, so we choose the $+$ sign

in the exponent.

We can recognize the equation (4.5) aa a 2D Helmholtz equation whose solution can be expressed as:

$$\psi(\mathbf{r}) = \sum_m C_m H_m^+(kr) e^{im\phi} \tag{4.7}$$

And for the $r \to \infty$ we get approximate behaviour:

$$H_m(kr) \xrightarrow{r\to\infty} \sqrt{\frac{2}{\pi kr}} exp\left[i\left(kr - \frac{(m+1/2)\pi}{2}\right)\right] \sim \frac{e^{ikr}}{\sqrt{r}} \tag{4.8}$$

SCATTERING REGION

In this case we consider the scattering area, where $V(r) \neq 0$. In this case we use the potential function $V(R)$ obtained in chapter 2 and numerically solve the 2D Schrodinger equation. To obtain the phase shift we match the wave function in the scattering region to the wavefunction in the far away region and use the optical theorem.

SCATTERING PROCESS

For the scattering process we have a wave function outside the scattering potential as:

$$\Psi(r,\theta) = e^{ikx} + f(\theta)\frac{e^{ikr}}{\sqrt{r}} \tag{4.9}$$

Now we expand:

$$e^{ikx} = e^{ikr\cos\theta} = \sum_m \epsilon_m i^m \cos(m\theta) J_m(kr) \tag{4.10}$$

where $\epsilon_m = 2$ for $m \neq 0$ and $\epsilon_0 = 1$.

Note: This looks very similar to the 3D case. The main difference is that in 2D case, the solution is a sum of cylindrical Bessel functions $J_m(kr)$ and $N_m(kr)$. In the 3D case, the solution is the sum of the spherical Bessel functions.

So the wave function looks like:

$$\Psi(r,\theta) = \sum_m^\infty \epsilon_m i^m \cos(m\theta) J_m(kr) \tag{4.11}$$

Now using asymptotic expressions for $r \to \infty$:

$$\begin{aligned} J_m(kr) &\xrightarrow{r\leftarrow\infty} = \sqrt{\frac{2}{\pi kr}} \cos\left(kr - \frac{m\pi}{2} - \frac{\pi}{4}\right) \\ N_m(kr) &\xrightarrow{r\leftarrow\infty} = \sqrt{\frac{2}{\pi kr}} \sin\left(kr - \frac{m\pi}{2} - \frac{\pi}{4}\right) \end{aligned} \tag{4.12}$$

The most general solution of the radial part is in the absence of potential is:

$$R(r) = A_m J_m(kr) + B_m N_m(kr) \tag{4.13}$$

For $r \to \infty$ the (4.13) has asymptotic form

$$R(r) = A_m \frac{1}{\sqrt{kr}} \cos\left[kr - \pi\frac{m+1/2}{2} + \delta_m\right] \tag{4.14}$$

Now equating equations (4.14) and (4.9) and using (4.10),(??) we obtain:

$$\begin{aligned} &\sum_m \epsilon_m i^m \sqrt{\frac{2}{\pi kr}} \cos(m\theta) \cos\left[kr - \pi\frac{m+1/2}{2}\right] + f(\theta)\frac{e^{ikr}}{\sqrt{r}} = \\ &\sum_m A_m \frac{1}{\sqrt{kr}} \cos\left[kr - \pi\frac{m+1/2}{2} + \delta_m\right] \cos(m\theta) \end{aligned} \tag{4.15}$$

Now this can be rewritten as:

$$\sum_m \epsilon_m i^m \sqrt{\frac{2\cos(m\theta)}{\pi kr}} \left[e^{i\left(kr - \pi\frac{m+1/2}{2}\right)} + e^{-i\left(kr-\pi\frac{m+1/2}{2}\right)} \right] + f(\theta)\frac{e^{ikr}}{\sqrt{r}} = \\ \sum_m A_m \frac{\cos(m\theta)}{\sqrt{kr}} \left[e^{i\left(kr-\pi\frac{m+1/2}{2}+\delta_m\right)} + e^{-i\left(kr-\pi\frac{m+1/2}{2}+\delta_m\right)} \right] \tag{4.16}$$

Now coefficients with e^{ikr} and e^{-ikr} must be equal. After some algebra and following[?] we get:

$$A_m = 2\epsilon_m \frac{i^m}{\sqrt{2\pi k}} e^{i\delta_m} \tag{4.17}$$

So the scattering amplitude is:

$$f(\theta) = \sqrt{\frac{1}{2\pi ik}} \sum_{m=0}^{\infty} \epsilon_m \cos(m\theta) \left[e^{2i\delta_m} - 1 \right] \tag{4.18}$$

So far, this is a general formula applicable to any kind of process.

CHAPTER 5

THE RADIATIVE QUENCHING H_2^+ ION ATOM COLLISIONS IN 2D SPACE

The analysis of the radiative processes is related to the analysis of the general scattering process. So we list those.

Typically for the scattering processes at this level, we can distinguish between the radiative and non-radiative processes.

Radiative processes involve emission of a photon and they typically mean Radiative Charge Transfer:

$A(n+1\,^1S)+B \longleftrightarrow A(n\,^1S)+B+\hbar\omega$

and Radiative Association:

$A(n+1\,^1S)+B \longleftrightarrow A(n\,^1S)B+\hbar\omega$.

For example, the simplest case of the radiative process is the collision of the two hydrogen atoms, in the process $H+H^+ \rightarrow H^+ + H + \hbar\omega$.

While the non-radiative process, with no photon emission, is a Charge Transfer:

$A(n+1\,^1S)+B(n\,^1S) \longleftrightarrow A(n\,^1S)+B(n+1\,^1S)$.

Radiative Quenching is an interaction between two atoms (or molecules), one being in excited state and the other in 'normal' ground state. During this process the excited atom emits a photon and drops to a ground state. The simplest such case is the collision of the two hydrogen molecules, in the process $H_2(2\,^2S) + H_2(1\,^2S) \rightarrow H_2(1\,^2S) + H_2(1\,^2S) + \hbar\omega$.

There are several theoretical approaches to this problem.[?],[?],[?]. While the problem has not been solved analytically, we will show that it can be solved numerically, to a desired precision. The radiative processes are driven by the interaction of the collision system with the radiation field. The direct change transfer is due to the transition between atomic (molecular) states due to the nuclear motion. Because the collision energy considered is low, typically only molecular states included are those which correspond to the initial $A\,^1\Sigma^+$ and final $X\,^1\Sigma^+$ channels.

Here we shall investigate the low energy collision process between the hydrogen atom and the hydrogen ion, in 2 dimension. We use fully quantum mechanical approach to calculate the cross section and the emission spectra of the reaction $H(2\,^2S)+H(1\,^1S) \rightarrow H(1\,^1S)+H(1\,^1S)+\hbar\omega$, formed by the quenching of the excited H atom by the approaching H atom, in 2D dimensions. To my knowledge, there is no experimental results related to the 2D problem. There are results for the 3D case, listed in[?] and references there.

In this calculation, the atoms are confined in 2 dimensions, while the radiation is emitted or absorbed in all 3D space. Therefore the photon can be emitted

in any direction and the potential felt by the incoming ion is the standard 3D Coulomb potential.

We will model this as a scattering problem, using a Born-Oppenheimer approximation and optical theorem. The Hamiltonian in this case will contain another term, namely the interaction of the radiation field with the electron

LENGTH GAUGE

The length gauge is a gauge transformation that replaces the vector potential for the field by the scalar potential for the quasi-static electric field[?] . In this gauge we take the Hamiltonian as: $H = \mathbf{p}^2/2m + V(\mathbf{r}) + e\mathbf{E}\mathbf{r}$. The length gauge is convenient since both the Coulomb and the external fields are represented by the scalar potentials, which are additive. In the presence of the radiation field, the length gauge is obtained by the gauge transformation of the vector potential $\mathbf{A}$, such that $\mathbf{A} \to \mathbf{A} + \nabla\chi$ where $\chi = -\mathbf{r} \cdot \mathbf{A}$.

In the length gauge, the interaction Hamiltonian is:

$$\begin{aligned} H_{int} &= -\sum_j \mathbf{r} \cdot \mathbf{E} \\ \mathbf{E} &= i \sum_{k\alpha} \left(\frac{2\pi ck}{V} \right)^{1/2} \hat{\epsilon}_{k\alpha} \left(a_{k\alpha} - a^\dagger_{k\alpha} \right) \end{aligned} \tag{5.1}$$

where $a_{k\alpha}$ and $a^\dagger_{k\alpha}$ are destruction and creation operators for the photon of momentum $\hbar k$ and polarization α respectively.

5.1 ELECTRONIC TRANSLATION FACTOR (ETF)[? ? ?]

The molecular approach to atomic collisions require the addition of the Electronic Translation Factor (ETF). Physically the reason for this factor is to ensure a Galilean invariance of the results. Which in turn means that the equations should be invariant to translations. Translation in this case corresponds to the movement of the molecules[?]. It has been shown[?] that an ETF does impact the cross section. The introduction of a switching function into the electron translation factor is relatively simple approach that greatly improves the accuracy of the cross section computation. Even though method of switching function is not a general one[?], it is well suited to the specially symmetric systems such as H_2^+.

5.2 RADIATIVE QUENCHING ANALYTICAL ANALYSIS

We start with the following Hamiltonian.

$$H = -\frac{1}{2\mu}\nabla^2_{\mathbf{R}} + H_{el}(\mathbf{R},\mathbf{r}) + H_{rad} + H_{int} \tag{5.2}$$

where $\mu = \frac{m_p\, m_e}{m_p + m_e}$, is the reduced mass, $\nabla_{\mathbf{R}}$ is the gradient operator for the relative nuclear motion. $H_{el}(\mathbf{R},\mathbf{r})$ is the fixed nuclei Hamiltonian for the electron, whose coordinate are labeled by $\mathbf{r}$. H_{rad} is the Hamiltonian of the radiation field, and H_{int} is the radiation-matter coupling. Since we are dealing with the interaction of an atom with the EM radiation, it is common to use the length

gauge.

So if we regard this process as a transition induced by the radiation field from the $A^1\Sigma_u^+$ state to of the H_2 molecule formed by the approaching H atom, to the $X^1\Sigma_g^+$ state in which the atoms separate.

Now we write the system wave function:

$$|\Psi\rangle = F_a(\mathbf{R})\chi_a(\mathbf{R},\mathbf{r})\,|0\rangle + \sum_{k\alpha} F_{k\alpha}(\mathbf{R})\chi_b(\mathbf{R},\mathbf{r})\,|k\alpha\rangle \tag{5.3}$$

where $\chi_a(\mathbf{R},\mathbf{r})$ and $\chi_b(\mathbf{R},\mathbf{r})$ are the eigenstates of the fixed position nuclei Hamiltonian H_{el} corresponding to the $A^1\Sigma_u^+$ and $X^1\Sigma_g^+$ state in body fixed frame respectively. The $F_a(\mathbf{R})$ and $F_{k\alpha}(\mathbf{R})$ are the amplitudes for the relative nuclear motion and $|0\rangle$ and $|k\alpha\rangle$ are the kets for the photon vacuum and single photon states. The ansatz (5.3) is valid at low speed collisions, where the other channels are inaccessible. In the adiabatic approximation (i.e. ignoring the non-adiabatic effects) the amplitudes $F_a(\mathbf{R})$ and $F_{k\alpha}(\mathbf{R})$ obey the set of coupled equations:

$$\left[-\frac{1}{2\mu}\nabla_R^2 + V_a(R) - E\right] F_a(\mathbf{R}) = \sum_{k\alpha} F_{k\alpha}(\mathbf{R})U_{k\alpha}(\mathbf{R}) \tag{5.4}$$

$$\left[-\frac{1}{2\mu}\nabla_R^2 + V_b(R) + \hbar\omega - E\right] F_{k\alpha}(\mathbf{R}) = F_a(\mathbf{R})U_{k\alpha}^\dagger(\mathbf{R}) \tag{5.5}$$

where

$$U_{k\alpha}(\mathbf{R}) = -i\left[\frac{2\pi ck}{V}\right]^{1/2} D(R)\hat{\mathbf{R}}\cdot\hat{\epsilon}_{k\alpha} \tag{5.6}$$

and $V_a(R), V_b(R)$ are the potential energy curves for the $A^1\Sigma_u^+$ and $X^1\Sigma_g^+$ states

respectively. $D(R)$ is the radial transitional dipole moment between them. E is the initial energy of the relative motions and ω is the angular frequency of the emitted photon. Now the next step is to solve this. We find the Green function for the equation (5.5) which satisfies the retarded boundary conditions so that $F_{k\alpha}$ contains only outgoing waves in the limit $R \to \infty$:

$$\left[-\frac{1}{2\mu}\nabla_R^2 + V_b(R) + \hbar\omega - E\right] G^+(\mathbf{R}, \mathbf{R}') = \delta^3(\mathbf{R}, \mathbf{R}') \tag{5.7}$$

and from the equation (5.7) we get:

$$F_{k\alpha}(\mathbf{R}) = \int d^3R' G^+(\mathbf{R}, \mathbf{R}') F_a(\mathbf{R}') U^\dagger_{k\alpha}(\mathbf{R}') \tag{5.8}$$

5.3 Solution Strategies

The main approaches to solving problems is to expand the wave function in the partial waves basis and use Born approximation.

Using partial waves we expand the incoming wave in the basis of spherical harmonics, and in the case of azimuthal symmetry to the basis of Legendre Polynomials. This in effect mean that we decompose each wave into its constituent angular momentum components and solving using boundary conditions.

Born approximation[?] treats a scattering potential as a perturbation to the incoming wave. In this case many partial waves contribute to scattering, so it is preferable to avoid angular momentum decomposition. The Born approximation is generally applicable either when the energy of the incoming particle(s)

is high or when the scattering potential is very weak.

5.3.1 USING PARTIAL WAVES

We can express this function in the partial waves bases. Since V_b contains no bound states we get for $\mathbf{R} = \mathbf{R}(R, \theta)$:

$$G^+(\mathbf{R}, \mathbf{R}') = \frac{\pi\mu}{k_b} \sum_{l=0}^{\infty} \sqrt{\frac{1}{2\pi}} P_l(\cos\theta) P_l^*(\cos\theta') \times \frac{f_l(k_b R_<) g_l^+(k_b R_>)}{RR'} \tag{5.9}$$

where $P_l(\cos\theta)$ are Legendre polynomials, also $\theta = 0$ part of the spherical harmonics: $P_l(\cos\theta) = Y_{l0}\theta, 0$.

The $f_l(R)$ is a regular solution of the homogeneous Schrodinger radial equation for the 2D case:[?] :

$$\frac{1}{R}\frac{d}{dR}\left(R\frac{d\, f_m(R)}{dR}\right) + \left\{k^2 - \frac{m^2}{R^2} - 2\mu\left[V_b(R) - V_b(\infty)\right]\right\} f_m(R) = 0 \tag{5.10}$$

$k \equiv \sqrt{2\mu[E - \hbar\omega - V_b(\infty)}$

where: The solution of the equation (5.10) are Bessel functions $J_m(kR)$ and $N_m(kR)$ with the asymptotic behaviour:

$$f_m(kR) \sim \sqrt{\frac{2}{\pi}} \cos\left[kR - \pi\frac{m + 1/2}{2}\right] \tag{5.11}$$

and $g_l^+(kR)$ is irregular solution with the boundary condition at large R.

$$g_m^+(kR) \sim \sqrt{\frac{2}{\pi}} \cos\left[kR - \pi\frac{m + 1/2}{2} + \delta_m\right] \tag{5.12}$$

and δ_m is a phase shift.

The total wave function (5.3) must be symmetric under the interchange of the H nuclei, so that $F_a(\mathbf{R}) = -F_a(-\mathbf{R})$ and $F_{k\alpha}(\mathbf{R}) = F_{k\alpha}(-\mathbf{R})$. Now we solve

equations (5.4) and (5.5) in the distorted wave approximation. Then $F_a(\mathbf{R})$ is the solution of the (5.4) with the coupling term set to be zero and it can be expressed in the form:

$$F_a(\mathbf{R}) = \sum_{m=1}^{\infty} P_m(\cos\theta)(2m+1)i^l\sqrt{\pi} \times \exp[i\delta_m]\frac{s_m(k_a\mathbf{R})}{k_a\mathbf{R}} \tag{5.13}$$

The asymptotic form for (5.13) is:

$$F_a(\mathbf{R}) \sim \frac{1}{\sqrt{2}}\left[e^{ik_az} - e^{-ik_az} + [f(\theta,\phi) - f(\theta-\pi,\phi+\pi)]\frac{e^{ik_aR}}{R}\right] \tag{5.14}$$

By inserting (5.13) and (5.9) into (5.8) we get the asymptotic form for the (5.8):

$$F_{k\alpha}(\mathbf{R}) \sim \frac{e^{ik_aR}}{R} f_{k\alpha}(\theta) \tag{5.15}$$

where:

$$f_{k\alpha}(\theta) = \sum_m \cos(l\,\theta)\left[\sum_{m=1}^{\infty}\frac{2\pi\mu}{k_ak_b}(2m+1)\left(\frac{\pi kc}{A}\right)^{1/2} e^{i\delta_j(b)}e^{i\delta_j(a)}i^{J+l-1}\right]\sqrt{2l+1)2\pi} \tag{5.16}$$

In this summation, the j is restricted to the odd integers, and

$$M_{m,m'}(k_a,k_b) = \frac{1}{\sqrt{k_a,k_b}}\int_0^{\infty} dR s_m(k_a,R)D(R)f_{m'}(k_b,R) \tag{5.17}$$

The cross section of the collision induced transition between the H atom and the H^+ ion is obtained by summing $|f_{k\alpha}(\theta)|^2$ over all final states that conserve energy with an initial state, and dividing the result with the flux of the incident channel.

The $H\,(2^1S) \rightarrow H\,(1^1S)$ is a linear combination of $A1\sigma_u^+$ and $X1\sigma_g^+$ states.

Since the excited gerade state is not allowed to make a radiative transition to a gerade ground state, the flux in the incident channel is twice the flux in the $A1\sigma_u^+$ channel.

So for the cross section we get:

$$\sigma = \int_0^{\omega_{max}} d\omega \frac{d\sigma}{d\omega} = \\ = \sum_\alpha \int \frac{d^2k}{(2\pi)^2} \frac{A}{2\mu k_a} \int d^2k_b \delta \left[\frac{k_b^2}{2\mu} - \frac{k_a^2}{2\mu} + \Delta E - \hbar\omega \right] |f_{k\alpha}(\theta)| \tag{5.18}$$

where

$$\frac{d\sigma}{d\omega} = \frac{8}{3} \left[\frac{\pi\mu}{k_a} \right]^2 \frac{1}{c^3} \omega^3 \sum_J \left[J M^2_{J,J-1}(k_a, k_b) + (J+1) M_{J,J+1}(k_a, k_b) \right] \tag{5.19}$$

ΔE is the energy of the transition at $R = \infty$ and ω_{max} is the maximum frequency of the emitted photon. Expression (5.18) is an equivalent expression to the Fermi's Golden Rule. Equation (5.19) provides the spectrum of the emitted radiation, in addition to the scattering cross section.

5.3.2 Optical Potential Method

The approximation that does not require the integration over the total spectrum is the optical potential method.

Again it is assumed that the scattering takes place at low energies, so that the system can be described by a wave function $\Psi(x,t)$ which is itself a solution of a Schrodinger equation $H|\Psi(t)\rangle = i\hbar\frac{\partial}{\partial t}|\Psi(t)\rangle$ where H is a Hamiltonian $H = T + V$. Then we borrow a concept from the optics, where there is a

concept of a Complex Refractive Index n. The real part of n describes how the light is transmitted and the imaginary part describes how the light is absorbed. So it the imaginary part that describes the effect of the scattering. We then express the potential $V = U + iW$ and the Schrodinger equation becomes $[H + U + iW]\,|\Psi(t)\rangle = i\hbar\frac{\partial}{\partial t}\,|\Psi(t)\rangle$. From this one gets the scattering cross section:

$$\sigma = \frac{k}{E}\int d^3R\,[-W(R)]\,|\psi(R)| \tag{5.20}$$

To derive it here we insert the equation (5.8) for the amplitude $F_{k\alpha}(\mathbf{R})$ into the equation (5.4) to obtain the equation for the amplitude $F_a(\mathbf{R})$

$$\left[-\frac{1}{2\mu}\nabla_R^2 + V_a(R) - E\right]F_a(\mathbf{R}) = \sum_{k\alpha} d^2R' G^+(\mathbf{R},\mathbf{R}')U^\dagger_{k\alpha}(\mathbf{R}')U_{k\alpha}(\mathbf{R})F_a(\mathbf{R}') \tag{5.21}$$

The right hand of (5.21) contains a complex, non-local potential

$$V(\mathbf{R},\mathbf{R}') = \sum_{k\alpha} G^+(\mathbf{R},\mathbf{R}')U^\dagger_{k\alpha}(\mathbf{R}')U_{k\alpha}(\mathbf{R}) \tag{5.22}$$

that arises because of the interaction of the electron with the vacuum. Now the real part of this potential induces the shift in the eigenvalue $V_a(R)$. Since the coupling on an electron with the radiation is weak, we can ignore it and consider only the imaginary part.

The imaginary part of $V(\mathbf{R},\mathbf{R}')$ is an absorptive potential, representing a process where electron in excited state emits a photon and decays to a ground state. This potential is non-local, as we take is for $R = \infty$. In the optical poten-

tial approximation, we take replace potential by the local one, whose range is limited to the scattering area. This potential is essentially classical.

Because the term $U^{\dagger}_{k\alpha}(\mathbf{R}^{'})U_{k\alpha}(\mathbf{R})$ appearing in equation (5.22) is real, the optical potential is proportional to the imaginary part of the retarded Green's function, which is expressed as:

$$\mathrm{Im}G^{+}(\mathbf{R},\mathbf{R}) = \pi \sum_{l=0}^{\infty} \cos(l\,\theta)\cos(l\,\theta^{'}) \int_{0}^{\infty} dk\,\delta\left[\frac{k^2}{2\mu} - \frac{k_a^2}{2\mu} + \hbar\omega - \Delta E\right] \frac{f_l(kR) f_l(kR^{'})}{R\,R^{'}} \tag{5.23}$$

This result is obtained using the spectral representation of the retarded Green's function and the identity $1/(x+i\epsilon) \to P/x - i\pi\delta(x)$ as $\epsilon \to 0$. Using (5.23) one obtains for the non-local optical potential:

$$V(\mathbf{R},\mathbf{R}^{'}) = \frac{i}{2\pi} \sum_{\alpha} \int d\Omega_k \int_{0}^{k_{max}} \sum_{l=0}^{\infty} \cos(l\,\theta)\cos(l\,\theta^{'}) \times \frac{\omega^3}{c^3} \frac{f_l(kR) f_l(kR')}{R\,R'} D(R) D(R') (\hat{\mathbf{R}} \cdot \epsilon_{k\alpha})(\hat{\mathbf{R}}^{'} \cdot \epsilon_{k\alpha}) \tag{5.24}$$

where $\omega(k) = k_\alpha/2\mu + \Delta E - k^2/\mu$. Now for the optical-potential approximation we make the semi-classical approximation that the values of k that give the largest contribution are given by:

$$\frac{k^2}{2\mu} \simeq= \Delta E + \frac{k_\alpha^2}{2\mu} + V_b(r) - V_a(r) \tag{5.25}$$

Now the frequency term $\omega^3 = |\Delta E(R)|^3$ can now be taken outside the integral.

Using the delta function expansion in 2 dimensions:

$$\delta^{(2)}\left(\mathbf{R},\mathbf{R}^{'}\right)=\sum_{l=0}^{\infty}\cos(l\,\theta)\cos(l\,\theta')\frac{\delta(R-R')}{R\,R'} \tag{5.26}$$

we get:

$$\begin{aligned} V_{opt}(\mathbf{R},\mathbf{R}) &\approx= \frac{i}{2}\delta^{(2)}\left(\mathbf{R},\mathbf{R}^{'}\right)A(R), \\ A(R) &= \frac{4}{3}D^2(R)\frac{|\Delta E(R)|^3}{c^3} \end{aligned} \tag{5.27}$$

and equation (5.24) becomes:

$$\left[-\frac{1}{2\mu}\nabla_R^2+V_a(R)-E\right]F_\alpha(\mathbf{R})=\frac{i}{2}A(R)F_\alpha(\mathbf{R}) \tag{5.28}$$

The cross section for the radiative quenching is given by:

$$\sigma=\frac{\pi}{k_a^2}\sum_{m=0}^{\infty}(2m+1)\left(1-e^{-4\eta_j}\right) \tag{5.29}$$

where η_j is the imaginary component of the phase shift of the Jth partial wave of the solution (5.24). The sum on J is restricted to the odd integers. Also because the right hand of (5.24) is small, we can use the distorted wave approximation to obtain the expression for the phase shift η_j

$$\eta_j=\frac{\pi\mu}{2k_a}\int_0^\infty dR\;|s_J\,(k_aR)|^2\,A(R) \tag{5.30}$$

5.3.3 CALCULATION

We use the code in appendixE for calculating the phase shift η, from the equation (5.30).

One has to pay attention when calculating the $D(R)$. Following[?] we have:

$$D(\vec{R}) = \langle \psi(\vec{r}) \,|\, (-1) \,|\, e \,|\, \vec{r} \,|\, \psi(\vec{r}) \rangle - |e|\vec{R} \tag{5.31}$$

Where the $\psi(\vec{r})$ is the electron eigenstate and $\vec{r}$ is the electron coordinate. From the symmetry argument we can deduce[?] that the components of $D(\vec{R})$ along the x axis vanis 2.1. So the remaining components is along the z axis, connecting the two nuclei. So we get:

$$D(R) = \langle \psi(\vec{r}) \,|\, (-1) \,|\, e \,|\, z \,|\, \psi(\vec{r}) \rangle - |e|R \tag{5.32}$$

We use the elliptical coordinates λ and μ from (3.2), (3.3), appendix C and figure 2.1. So to solve the integral (5.32) we start from the original definition on the elliptic coordinates

$$z = \frac{R}{2}\cosh\eta\cos\nu \quad y = \frac{R}{2}\sinh\eta\sin\nu \Rightarrow \quad \lambda = \cosh\eta; \;\; \mu = \cos\nu \Rightarrow z = -\frac{R}{2}\lambda\mu \tag{5.33}$$

and divide the z axis into 3 regions (avoiding the singularities at -1 and 1).

$$\begin{aligned} &1 : -\infty < z \leq -1 : \; \eta > 0, \nu = \pi :\Rightarrow \lambda > 1, \mu = -1 \\ &2 : -1 < z \leq 0 : \; \eta = 0, \nu = [0, \pi] :\Rightarrow \lambda = 1, \mu = [-1, 1] \\ &3 : 1 < z < \infty : \; \eta > 0, \nu = 0 :\Rightarrow \lambda > 1, \mu = 1 \end{aligned} \tag{5.34}$$

So finally for the $D(R)$ we have 3 integrals:

$$\int_{-\infty}^{-1} d\lambda\ [L(\lambda)M(\mu=-1)]^* \left(-\frac{R}{2}\right) \lambda\, L(\lambda)M(\mu=-1)$$

$$\int_{-1}^{1} d\mu\ [L(\lambda=1)M(\mu)]^* \left(-\frac{R}{2}\right) \mu\, L(\lambda=1)M(\mu) \tag{5.35}$$

$$\int_{1}^{\infty} d\lambda\ [L(\lambda)M(\mu=1)]^* \left(-\frac{R}{2}\right) \lambda\, L(\lambda)M(\mu=1)$$

Here is the graph of the Transition Dipole Moment between the states $1s^+$ and $2p^+$.

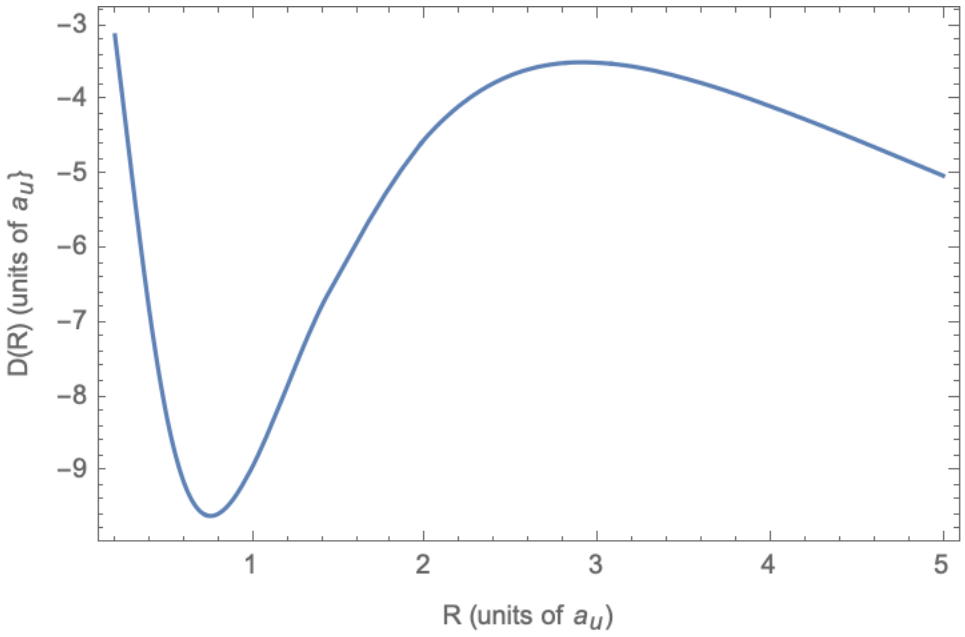

We then use transition dipole values to compute the cross section.

The Mathematica code used for calculation is shown n appendix E.

5.3.4 RESULT AND DISCUSSION

In fig we plot the calculated cross section for process. The cross section is obtained using the calculation in section 5.3.3. The energy range is in

CHAPTER 6

RADIATIVECHARGE TRANSFER

In this section we describe the charge transfer in 2 dimension, analogous to the approach we tok in chapter 5

6.0.1 APPLICATION OF THE BORN-OPPENHEIMER (BO) APPROXIMATION

Following[?] employ the Born-Oppenheimer (BO) approximation. We expand the scattering wave function in the terms of BO wave functions, adding the electronic translation factor. If we set $\chi_i^a(\mathbf{R})$ to the be wave function of the nuclear motion in the electronic state i, we get for the wavefunction:

$$\Psi(\mathbf{r},\mathbf{R}) = \sum_i exp\left[\frac{1}{\mu}\mathbf{S}\cdot\nabla_R\right]\phi(\mathbf{r},\mathbf{R})\chi_i^a(\mathbf{R}) \tag{6.1}$$

with μ being the reduced mass, and

$$S = \frac{1}{2}f_i(\mathbf{r},\mathbf{R})\mathbf{r} \tag{6.2}$$

where f_is are the switching functions that incorporate the molecular character of the ETF. The equations for the $\chi_i^a(\mathbf{R})$ can be obtained in a matrix form:

$$\left\{-\frac{1}{2\mu}\left[\underline{I}\nabla_R - i(\underline{\mathbf{P}} + \underline{\mathbf{A}})\right]^2 + \underline{V}\right\}\underline{\chi}^a(\mathbf{R}) = E\underline{\chi}^a(\mathbf{R}) \tag{6.3}$$

with:

$$\begin{aligned}
\mathbf{P}_{ij} &= \langle\phi_i \,|\, -i\nabla_R \,|\, \phi_j\rangle \\
\mathbf{A}_{ij} &= i(E_i - E_j)\,\langle\phi_i \,|\, \mathbf{S} \,|\, \phi_j\rangle \\
V_{ij}(R) &= \delta_{ij}V_i(R)
\end{aligned} \tag{6.4}$$

where E is the energy of the nuclear motion in the center of mass frame, and $\underline{I}$ is the identity matrix. The matrix $\mathbf{P}_{ij}$ represents the non-adiabatic coupling, the $\mathbf{A}_{ij}$ is the ETF correction, and the $V_i(R)$ is the potential energy of the ith Born-Oppenheimer state.

6.1 Calculation of Radiative charge transfer

Following the similar approach as in chapter 5 the radiative charge transfer cross-section can be calculated using the formula (5.18) for σ with M calculated using formula (5.17), where the k_a and k_b are the wave numbers of the initial and final state.

The partial waves $f_j(kR)$ and $s_j(kR)$ are the regular solutions of the homogeneous radial equations.

$$\left\{\frac{d^2}{dR^2} - \frac{J(J+1)}{R^2} - 2\mu\left[V_a(R) - V_b(\infty)\right\} + k_a^2\right\}s_j(k_aR) = 0 \tag{6.5}$$

and

$$\left\{\frac{d^2}{dR^2} - \frac{J(J+1)}{R^2} - 2\mu\left[V_b(R) - V_a(\infty)\right\} + k_b^2\right\}f_j(k_bR) = 0 \tag{6.6}$$

with $V_a(R)$ and $V_b(R)$ being the potential energy curves of the final ground state and the initial excited state, respectively. The k_a and k_b are the wave numbers, given by:

$$\begin{aligned} k_b &= \sqrt{2\mu\left[E - \hbar\omega - V_b(\infty)\right]} \\ k_a &= \sqrt{2\mu\left[E - V_a(\infty)\right]} \end{aligned} \tag{6.7}$$

where ω is the angular frequency of the emitted photon, E is the total collision energy in the center of mass frame.

As a second order equation, the solution requires two initial conditions, either in the form of function value at the ends of the interval, or value of the function and its derivative at some point. Now, this partial wave represents an incoming particle (electron) and thus the function $f(kR)$ is defined on the infinite interval and it is oscillatory for large values of kR. Because of that, it is impossible to specify a boundary condition for value of $f(kR)$ at infinity. So the boundary conditions have to be in the form of the value of function at some point and the value of the derivative at the same point.

In this calculation, we assume that for $kR \to 0$, the function $f(kR)$ is finite and 'well behaving', so the appropriate boundary conditions seem to be:

$$\text{For } kR \to 0,\ f(kR) = 1\,;\ f'(kR) = 0 \tag{6.8}$$

The Mathematica code for the $f(kR)$ is in appendix TODO: add code.

Following the approach in the[?] I apply a semi-classical approach to the system of two H_2^+ molecules. In this approach, I assume that a photon is emitted

with energy equal to the energy difference between two Born-Oppenheimer potential surfaces, at the distance where the transition occurs. This leads to the Local Optical Potential Method, and following the semi-classical approach, the total rate is estimated as a classical integral over all localized transitions.

The cross section of the spontaneous radiative association is given by[?] . This can also be derived using the Fermi's Golden Rule (which is actually published by Dirac 20 years before Fermi)[?] :

$$\sigma_{CT} = \int_0^{\omega_{max}} d\omega \, \frac{d\sigma}{d\omega}$$

where :

$$\sigma_{sp}(k) = \sum_J \sum_n \frac{64}{3} \frac{\pi^5 \nu^3}{c^3 k^2} \left[(J+1) M^2_{J+1,J} + J \, M^2_{J-1,J} \right] \tag{6.9}$$

The sum extends over the rho-vibrational quantum numbers n and angular momentum J of the H_2^+ ion. Due to the topological constraints the direction of J remains fixed, and only its magnitude changes. As expected, for the ground state we have $J = 0$.

The $M_{J,J'}$ is an overlap integral defined by:

$$M_{J,J'} = \int_0^\infty dR \, f_j(kR) D(R) \phi^n_{J'}(R) \tag{6.10}$$

where $f_j(kR)$ is a partial wave defined above.

VIBRATIONAL LEVELS

The $\phi_{J',n}(R)$ represents the vibrational eigenfunction of the ground state $X^2\Sigma^+$ with the energy $\epsilon_n J$. TODO: Show picture. Given the nature of the problem 2D, the ground state has the $J = 0$. So the differential equation for the $\phi_{0,n}(R)$, in the potential well, is:

$$\phi''_{0,n}(R) + [E(R) + V(R)]\,\phi(R)_{0,n} = \epsilon_n \phi(R)_{0,n} \tag{6.11}$$

Of course the solution to this equation can only be calculated numerically (appendix TODO: show the Mathematica code.). To solve the equation one must set the boundary conditions to $\phi(R)_{0,n} \Rightarrow 0, \phi(R)'_{0,n}$ for $R \Rightarrow 0$. For actual numerical evaluation, the important boundary condition is the value of $\phi(R \approx 0)_{0,n}$. With these boundary conditions set, the values of ϵ_n must satisfy the boundary condition on the other side of the potential well, namely that the $\phi(R)_{0,n}$ remains bounded, which translates into: $\phi(R)_{0,n} \Rightarrow 0$ for $R \Rightarrow \infty$.

So calculations show (TODO: Verify) that there are

DIPOLE TRANSITION IN 2 DIMENSION

The $D(R)$ is the transition dipole moment between $X^2\Sigma^+$ and $A^2\Sigma^+$,

$$D(R) = \langle \psi_1(R) \,|\, r_1 + r_2 \,|\, \psi_0(R) \rangle \quad \text{where in our case :} \tag{6.12}$$

$$r_1 + r_2 = \lambda\, R$$

Now the 2 dimension case comes into effect. I consider the case where the particle (electron in this case) is confined in 2 dimensions, but where the un-

derlying space is still 3 dimensional, Euclidean. Thus while particle's movement is confined in 2D, it can radiate photons in any direction in 3D.

TODO: Add appendix for the radiation in 1D and 2D.

With the separation of variable, the solution is a product of two function. So the integral above come t0o:

$$D(R) = \int_{-1}^{1}\int_{1}^{\infty} d\mu\, d\lambda\, M_u(\mu)L_u(\lambda)\lambda R M_g(\mu)L_g(\lambda) \tag{6.13}$$

where $M_u L_u$ and $M_g L_g$ are the odd/even solutions to the original Schrodinger equation (5.2).

Since the functions $M(\mu)$ and $L(\lambda)$ do not exist in the closed form, the dipole integral (6.13) is numerically calculated using Wolfram Mathematica. First the two Mathematica modules (functions) are created, which solve the equations $L(\lambda)$ and $M(\mu)$, as function of the internuclear distance R and corresponding variables. Then the second module calculates the integral above, as the function of R.

The Mathematica code for the dipole is in appendix TODO: add code and indicate that I wrote it. :)

From the table TODO: add reference one could calculate the spectrum of these transitions. For the electron to transition from $A^2\Sigma^+$ to $X^2\Sigma^+$ level, it needs to emit photon $\Delta E \approx -3.2\, au = 0.1176eV$, so the corresponding wavelength is $\lambda \approx 380\, nm$ TODO: Verify the numbers. TODO: verify the depth of the potential well compared to the paper?

TODO: Possible spectrum of such transitions

DISTORTED WAVE APPROXIMATION

The distorted wave Born approximation (DWBA) is an extension to the (first) Born approximation in scattering processes. Starting from the Schrodinger equation for the scattering problem, we solve it by method of Green's function

$$\left[-\frac{\hbar^2}{2m}\nabla^2 + V(\mathbf{r})\right]\psi_k(\mathbf{r}) = E\psi_k(\mathbf{r}) \tag{6.14}$$

with $V(\mathbf{r}) = 0$ except in the target region $\Longrightarrow$

The energy E is the energy of the incident plane wave, $E = \hbar^2 k^2/2m$. Applying the Green's function

$$\left[\frac{\hbar^2}{2m}\nabla^2 + E\right] G_0(\mathbf{r}, \mathbf{r}^{'}|E) = V(\mathbf{r})\psi_k(\mathbf{r}) \tag{6.15}$$

we get the integral form of the Schwinger-Lippmann equation:

$$\psi_k^{'}(\mathbf{r}) = \psi_k(\mathbf{r}) + \int d^3r^{'}\, G_0(\mathbf{r}, \mathbf{r}^{'}|E)V(\mathbf{r}^{'})\psi_k^{'}(\mathbf{r}) \tag{6.16}$$

The scattering amplitude is given by[?]

$$f_k(\mathbf{r}) = -\frac{2m}{\hbar^2}\frac{1}{4\pi}\int d^3r^{'}\, e^{-i\mathbf{k}\mathbf{r}^{'}} V(\mathbf{r}^{'})\psi_k^{'}(\mathbf{r}^{'}) \tag{6.17}$$

Since the Schwinger-Lippmann equation (6.16) is unsolvable, the first Born approximation assumes that the scattered field is small when compared to the incident field. Therefore it treats the scattered way as a perturbation. As the

$0-th$ order the scattered wave is an unperturbed incident plane wave:

$$\psi_0^{'}(\mathbf{r}) = e^{i\mathbf{kr}} \tag{6.18}$$

and then the equation (6.16) is solved iteratively:

$$\psi_{n+1}^{'}(\mathbf{r}) = e^{i\mathbf{kr}} + \int d^3r^{'}\, G_0(\mathbf{r},\mathbf{r}^{'}|E)V(\mathbf{r}^{'})\psi_k^{'}(\mathbf{r}) \tag{6.19}$$

So if we expand the wave function in the powers of the interaction potential V we get:

$$\begin{aligned}
\psi_k^{'} &= \psi_{\mathbf{k}}^{'(0)} + \psi_{\mathbf{k}}^{'(1)} + \psi_{\mathbf{k}}^{'(2)} + \ ... \\
&= \psi_{\mathbf{k}}^{'(0)} + G_0V\psi_{\mathbf{k}}^{'(0)} + G_0VG_0V\psi_{\mathbf{k}}^{'(0)} + \ ... \qquad (6.20) \\
&= (1+G_0T)\psi_{\mathbf{k}}^{'(0)} \qquad \text{with } T = V + G_0V + ... = \frac{1}{1-VG_0}
\end{aligned}$$

The equation (6.20) represents a scattering process where incident particle undergoes multiple scattering events from the potential. Since this makes the calculations very complicated, only the first iteration of the series is takes into account and the matrix T is approximated by the potential V. This first order term in which the exact wave function $\psi_{\mathbf{k}}^{'}(\mathbf{r})$ is replaced by the plane wave $e^{i\mathbf{kr}}$ is the First Born Approximation. It is very useful, however it is not always valid and one way to extend its validity is the DWBA.

In the DWBA, we do not assume any more that the scattered field is small compared to the incident field. So in this case, it is possible to generalize the Born approximation. The free space zero potential $V_0(\mathbf{r}) = 0$ is replaced by the non-trivial reference potential $V_1(\mathbf{r}) = 0$. It is assumed that the scattered wave

function $\psi_{\mathbf{k}}^{'1}$ due to this potential is known, either analytically or numerically as a solution to the following Schwinger-Lippmann equation:

$$\psi_{n+1}^{'}(\mathbf{r}) = e^{i\mathbf{kr}} + \int d^3r^{'}\, G_0(\mathbf{r}, \mathbf{r}^{'}|E) V_1(\mathbf{r}^{'}) \psi_k^{'1}(\mathbf{r}) \tag{6.21}$$

Then the interaction potential is treated as a perturbation to the reference potential V_1, i.e:

$$V(\mathbf{r}) = V_1(\mathbf{r}) + \delta V(\mathbf{R} \quad \text{with} \quad |\delta V| << |V_1| \tag{6.22}$$

So in the DWBA the scattering field is determined by applying the Born approximation:

$$\psi^{'}(\mathbf{r}) = \psi^{'1}(\mathbf{r}) + \int d^3r^{'}\, G_0(\mathbf{r}, \mathbf{r}^{'}|E) V_1(\mathbf{r}^{'}) \psi_k^{'1}(\mathbf{r}) \tag{6.23}$$

to the scattered wave $\psi^{'}(\mathbf{r})$. This distorted wave is the solution of the outgoing-wave Schrodinger equation:

$$\left[\frac{\hbar^2}{2m}\nabla^2 - V_1(\mathbf{r}) + E\right] \psi^{'1}(\mathbf{r}) = 0 \tag{6.24}$$

where we can use the Green's function method.

To satisfy the boundary conditions, the asymptotic form of the $\psi^{'1}(\mathbf{r})$ for $r \rightarrow \infty$ is:

$$\psi^{'1}(\mathbf{r}) \rightarrow e^{i\mathbf{kr}} + \frac{1}{r} e^{ikr} f_k^1(\theta) \tag{6.25}$$

where the scattering amplitude is:

$$f_k^1(\theta) = -\frac{2m}{\hbar^2}\frac{1}{4\pi}\int d^3r^{'}\, e^{-i\mathbf{kr}^{'}} V_1(\mathbf{r}^{'}) \psi_k^{'1}(\mathbf{r}^{'}) \tag{6.26}$$

This would be the scattering amplitude if the potential V_1 were the only poten-

tial present. The total scattering amplitude is the sum:

$$f_k(\theta) = f_k^1(\theta) + \delta f_k(\theta) \tag{6.27}$$

and $\delta f_k(\theta)$ is calculated in the Born approximation:

$$\delta f_k(\theta) \simeq -\frac{2m}{\hbar^2}\frac{1}{4\pi}\int d^3r'\, \psi_{k'}^{'1(-)*}(\mathbf{r}')V_1(\mathbf{r}')\psi_k^{'1}(\mathbf{r}') \tag{6.28}$$

The $\psi_{k'}^{'1(-)*}$ is the known incoming wave, corresponding to the reference potential V_1 (i.e. solution of the Schrodinger equation) .

The condition for the (6.28) to be a good approximation is for the $\delta V(\mathbf{r})$ to be sufficiently small. What that means is that possible additional scattering does not modify significantly the wave function.

CHAPTER 7

CONCLUSION

In this thesis, we investigated the scattering processes for particles in 2 dimensions. In Introduction we researched and discussed the application of the 2 dimensional materials, current and some possible future ones. We also discussed the applications of the 2D processes for Quantum Computing. Following the Introduction we focused on the hydrogen molecular ion H_2^+. We recalculated the existing result in 3 dimension. Then we applied the same technique to calculate the energy leves of the H_2^+ butIn chapters 3, 4 we used the results from the chapter 2 to calculat the cross section for the Radiative Quenching and Radiative Transfer respectively.

The references contain books and articles used to support the above investigation and calculation. * Copying from one place is plagiarism, copying from multiple places is research

APPENDIX A

CENTER OF MASS AS A PLANE WAVE

Take the isolated system of 2 interacting spinless particles. The particles are of masses m_1 and m_2 and are located at positions $\mathbf{r}_1$ and $\mathbf{r}_2$. The potential energy of the particles depends only on their relative position $\mathbf{r}_1 - \mathbf{r}_2$. The Langrangian of this system can be written as:

$$L = T - V = \frac{1}{2}m_1 \cdot r_1^2 + \frac{1}{2}m_2 \cdot r_2^2 + V(\mathbf{r}_1 - \mathbf{r_2}) = \frac{1}{2}M \cdot R^2 + \frac{1}{2}\mu \cdot r^2 + V(\mathbf{r}) \quad \text{(A.1)}$$

where

$M = m_1 + m_2$ is a total mass of the system

$\mu = \dfrac{m_1 m_2}{m_1 + m_2}$ is a reduced mass of the system

$\mathbf{R} = \dfrac{m_1\mathbf{r}_1 + m_2\mathbf{r}_2}{m_1 + m_2}$ are the coordinates of the center of the mass of the system, and

$\mathbf{r} = \mathbf{r}_1 - \mathbf{r}_2$ are the relative coordinates.

(A.2)

with:
$p_i = \frac{\partial L}{\partial q_i}$ we define

$$\mathbf{P} = M \cdot \mathbf{R} \quad \text{and } \mathbf{p} = \mu \cdot \mathbf{r} \text{ and we obtain} \tag{A.3}$$

$$\cdot\mathbf{P} = 0 \quad \cdot\mathbf{p} = -\nabla V \mathbf{r}$$

Now using the variables $\mathbf{P}, \mathbf{R}, \mathbf{p}, \mathbf{r}$ we get for the Hamiltonian:

$$H = \frac{P^2}{2M} + \frac{p^2}{2\mu} + V(\mathbf{R}) = H_{CM} + H_r \tag{A.4}$$

The first term represents the motion of the center of the mass, which is a uniform inertial motion, since $\cdot\mathbf{P} = 0$. The other terms represent the energy associated with the motion relative to the center of the mass. Now if we choose the inertial frame in which the center of the mass is at rest, we get the Hamiltonian to reduce to H_r, representing the motion of a single, fictitious particle in an external potential.

Now transitioning to a quantum case. The variables $H, \mathbf{P}, \mathbf{R}, \mathbf{p}, \mathbf{r}$ become operators, with the usual commutation relations:

$$[R_i, P_j] = [r_i, p_j] = i\delta_{ij} \text{ and } [R_i, p_j] = [r_i, P_j] = 0 \implies$$
$$[H_{cm}, H_r] = 0,\ [H_r, H] = 0\, [H_{CM}, H] = 0 \tag{A.5}$$

Since all the Hamiltonians commute, there exists a common eigenbasis in some state space E of H, H_{CM}, H_r. We can express the space E as a tensor product of spaces E_R and E_{cm} with $E = E_{CM} \otimes E_r$. The operators $\mathbf{P}, \mathbf{R}$ operate in space E_{CM} and operators $\mathbf{p}, \mathbf{r}$ operate in E_r space. From the La-

grangian and the Hamiltonian above we observe that the motion of the center of mass and the relative motion are completely independent of each other.

$$H_{CM}\left|\chi\right\rangle = E_{CM}Ket\chi \quad H_r\left|\omega\right\rangle = E_rKet\omega$$

$$H\left|\phi\right\rangle = (H_{CM}+H_r)(\left|\chi\right\rangle \otimes Ket\omega) = H_{CM}(\left|\chi\right\rangle \otimes Ket\omega) + H_r(\left|\chi\right\rangle \otimes Ket\omega) = (E_{CM}+E_r)(\left|\chi\right\rangle \otimes Ket\omega \tag{A.6}$$

Expressing the expressions above in coordinate representation, we have:

$$\phi(\mathbf{R},\mathbf{r}) = \chi(\mathbf{R})\omega(\mathbf{r})$$

$$H_{CM}\chi(\mathbf{R}) = E_{CM}\chi(\mathbf{R}) \quad H_r\omega(\mathbf{r}) = E_r\omega(\mathbf{r}) \tag{A.7}$$

$$-\frac{\hbar_R^2}{2M}\nabla^2\chi(\mathbf{R}) = E_{CM}\chi(\mathbf{R}) \quad -\frac{\hbar^2}{2M}\nabla_r^2\omega(\mathbf{r}) = E_r\omega(\mathbf{r})$$

So we can solve for $\chi(\mathbf{R})$ to obtain:

$$\chi(\mathbf{R}) = \frac{1}{(2\pi\hbar)^{3/2}}e^{\frac{i}{\hbar}\sqrt{2ME_{CM}}\mathbf{R}} \tag{A.8}$$

APPENDIX B

MATHEMATICA CODE FOR CALCULATING THE EIGENVALUES FOR THE H2 ION IN 3 DIMENSIONS

This is a fairly simple program which illustrates the power of Mathematica (and similar) mathematical applications. Following the derivation in chapter 1, we are left with two differential equations $M(\mu)$ and $L(\lambda)$. Each equation depends on two parameters $p^2 = -\frac{1}{4}R^2E$ where E is the electron energy and separation constant A.

We then create a array of values of R (nuclear distance), and for each value or F calculate eigenvalues of the equations (2.28) and (2.33), as a functions of p and A. Interpolate and the intersection of the functions of p and A provides an eigenvalue.

The last step is to add nuclear potential energy $1/R$, tabulate and plot the function.

```
(* Matrix dimensions *)
numCoefficents := 10;

numInterPoints := 20;

d[m_, n_] := KroneckerDelta[m, n];

lP[n_, x_] := LegendreP[n, x];

mSum[n_, x_] := (-n (n + 1) lP[n, x] + p^2 x^2 lP[n, x]);

mSumExpanded[m_, n_] := (-2 n (n + 1))/(2 n + 1) + p^2 (2 (2 n^2 + 2 n - 1))/((2 n + 3) (2 n + 1) (2 n - 1)) d[m, n] +
    p^2 (2 (n + 1) (n + 2))/((2 n + 1) (2 n + 3) (2 n + 5)) d[m, n + 2] + p^2 (2 n (n - 1))/((2 n + 1) (2 n - 1) (2 n - 3)) d[m, n - 2];

lSumExpanded[m_, n_] :=
  (-2 p n (2 n + 1) - (2 p - 1) n^2 + (-2 p + 2 R) (2 n + 1) + (-4 p + 1) n + (-2 p - p^2 + 2 R))
    d[m, n] + (2 p n (n + 1) - (-2 p + 2 R) (n + 1)) d[m, n + 1] +
   (2 p n^2 + (2 p - 1) n (2 n - 1) - (-2 p + 2 R) n + (4 p - 3) n) d[m, n - 1] +
   (-(2 p - 1) n (n - 1)) d[m, n - 2];

tableEofR = {};


allRs = Table[i, {i, 0.2, 5, 0.2}];
allRs  = Join[allRs, Table[i, {i, 5.5, 9, 0.5}]];

CalcE[radius_, max_, np_] := Module[{matrixM, matrixL, ee, q,
   pe, rm, pMax, pMin, pStep, eigenM, eigenL, pgrid, mFunc, lFunc},

    (* m = rows, n = columns.
     Sums go from 0 (zero), matrix indices go from 1
   *)


  (* M matrix *)
  matrixM = Table[0, {i, 1, max}];
  Do[
   matrixM[[m + 1]] = Table[mSumExpanded[m, n] (2 m + 1)/2, {n, 0, max - 1}],
   {m, 0, max - 1}
  ];
```

```
(* L Matrix  For Power series solution *)

matrixL = Table[0, {i, 1, max}];

Do[
 matrixL[[m + 1]] = Table[lSumExpanded[m, n], {n, 0, max - 1}],
 {m, 0, max - 1}
] ;

q = 2.;
pMax = 2. q radius / 2. + 1.;
pMin = radius / 2.;
pStep = (pMax - pMin) / np;

(*Output *)

(* {p, eigenvalue @ p } *)
eigenM = Table[0, {i, 1, np}, {j, 1, 2}];
eigenL = Table[0, {i, 1, np}, {j, 1, 2}];
pgrid = Table[pMin + (i - 1) * pStep, {i, 1, np}];

rm[x_] := If[Im[x] ≠ 0, 10^-99, x];

Do[
 eigenM[[i]][[2]] =
  Sort[Map[rm, Eigenvalues[N[matrixM /. p → pgrid[[i]], 10.]]], Greater][[1]];
 eigenM[[i]][[1]] = pgrid[[i]];
 eigenL[[i]][[2]] = Sort[Map[rm,
     (Eigenvalues[N[matrixL /. {R → radius, p → pgrid[[i]]}, 10.]] (-1))]][[1]];
 eigenL[[i]][[1]] = pgrid[[i]],
 {i, 1, np}
] ;

(* Now Interpolation *)

mFunc = (eigenM // Interpolation) ;
lFunc = (eigenL // Interpolation) ;

pe = x /. FindRoot[mFunc[x] == lFunc[x], {x, radius}];
```

```
  ee = -4 (pe/radius)^2;
  ee
 ]


(* Syntax:
    [E(R), E(R)+1/R] = CalcE[1,numCoefficents, numInterPoints]
*)

Energies := CalcE[#, numCoefficents, numInterPoints] & ;
Plot[{Energies[r], Energies[r] + 1/r}, {r, 0.1, 10},
 AxesOrigin → {0, 0}, PlotLabels → {E (R), E (R) + 1/R}]
```

Out[117]=

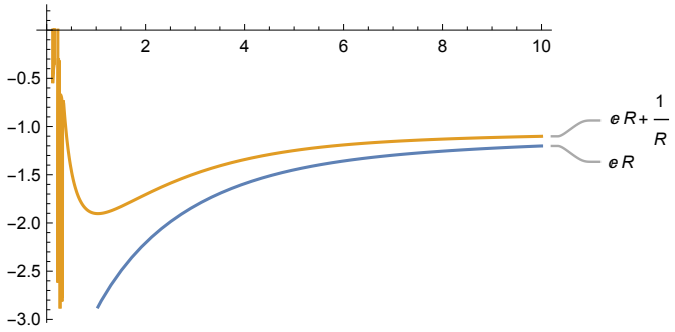

APPENDIX C

HYDROGEN ION IN 2 DIMENSION EQUATION, DERIVATION

$$\left(-\frac{1}{2}\nabla^2 - \frac{1}{r_a} - \frac{1}{r_b}\right)\psi = E\,\psi \tag{C.1}$$

As illustrated by the figure 3.1, we express equation (3.1) in the elliptical coordinates, and by setting the x axis to be perpendicular to the internuclear axis, we have the nuclei at: $y = \pm\frac{R}{2}$, R being the distance between nuclei. So in 2D elliptic coordinates, λ, μ we have

$$\lambda = (r_a + r_b)/R; \qquad \mu = (r_a - r_b)/R$$

$$\lambda = (r_a + r_b)/R; \qquad \mu = (r_a - r_b)/R \tag{C.2}$$

where $\lambda \in [1, \infty]$, $\mu \in [-1, 1]$ and

$$r_a = \frac{R}{2}(\lambda + \mu) \qquad r_b = \frac{R}{2}(\lambda - \mu)$$

Plug the variables λ and μ into the equation $(\mathrm{C}.1)$ we get by using 3D elliptic

cylindrical coordinates[?] .

$$\nabla^2 = \frac{4}{R^2(\lambda^2-\mu^2)}\left[\sqrt{\lambda^2-1}\frac{\partial}{\partial\lambda}\left(\sqrt{\lambda^2-1}\frac{\partial\psi}{\partial\lambda}\right)+\sqrt{1-\mu^2}\frac{\partial}{\partial\mu}\left(\sqrt{1-\mu^2}\frac{\partial\psi}{\partial\mu}\right)\right] = \frac{4}{R^2(\lambda^2-\mu^2)}\left[(\lambda^2-1)\frac{\partial^2\psi}{\partial\lambda^2}+\lambda\frac{\partial\psi}{\partial\lambda}+(1-\mu^2)\frac{\partial^2\psi}{\partial\mu^2}-\mu\frac{\partial\psi}{\partial\mu}\right] \tag{C.3}$$

So the equation transforms to (with $\psi = \psi(\lambda,\mu)$:

$$-\frac{1}{2}\frac{4}{R^2(\lambda^2-\mu^2)}\left[(\lambda^2-1)\frac{\partial^2\psi}{\partial\lambda^2}+\lambda\frac{\partial\psi}{\partial\lambda}+(1-\mu^2)\frac{\partial^2\psi}{\partial\mu^2}-\mu\frac{\partial\psi}{\partial\mu}\right]-\frac{2}{R(\lambda+\mu)}\psi-\frac{2}{R(\lambda-\mu)}\psi = E\psi \tag{C.4}$$

or

$$-\frac{1}{2}\frac{4}{R^2(\lambda^2-\mu^2)}\left[(\lambda^2-1)\frac{\partial^2\psi}{\partial\lambda^2}+\lambda\frac{\partial\psi}{\partial\lambda}+(1-\mu^2)\frac{\partial^2\psi}{\partial\mu^2}-\mu\frac{\partial\psi}{\partial\mu}\right]-\frac{4}{R}\frac{\lambda}{\lambda^2-\mu^2}\psi = E\psi \tag{C.5}$$

We assume that the total electronic wavefunction can be written as the product of two functions:

$$\psi(\lambda,\mu) = F(\mu)L(\lambda) \tag{C.6}$$

we obtain from $(\mathrm{C}.5)$

$$\frac{2}{R^2(\lambda^2-\mu^2)}\left[(\lambda^2-1)F\frac{\partial^2 L}{\partial\lambda^2}+\lambda F\frac{\partial L}{\partial\lambda}+(1-\mu^2)L\frac{\partial^2 F}{\partial\mu^2}-\mu L\frac{\partial F}{\partial\mu}\right]+\frac{4}{R}\frac{\lambda}{\lambda^2-\mu^2}FL+EFL = 0 \Rightarrow$$

$$(\lambda^2-1)\frac{1}{L}\frac{\partial^2 L}{\partial\lambda^2}+\frac{\lambda}{L}\frac{\partial L}{\partial\lambda}+(1-\mu^2)\frac{1}{F}\frac{\partial^2 F}{\partial\mu^2}-\frac{\mu}{F}\frac{\partial M}{\partial\mu}+2R\lambda+\frac{R^2}{2}E(\lambda^2-\mu^2) = 0 \tag{C.7}$$

Setting $p^2 = \frac{R^2}{2}E$ and rearraging:

$$(\lambda^2-1)\frac{1}{L}\frac{\partial^2 L}{\partial\lambda^2}+\frac{\lambda}{L}\frac{\partial L}{\partial\lambda}+2R\lambda+\frac{R^2}{2}E\lambda^2+$$
$$(1-\mu^2)\frac{1}{F}\frac{\partial^2 F}{\partial\mu^2}-\frac{\mu}{F}\frac{\partial M}{\partial\mu}-\frac{R^2}{2}E-\mu^2=0 \tag{C.8}$$

We can conclude that both equations for λ and μ must be equal to the separation constant A. So it follows that

$$(\lambda^2-1)\frac{\partial^2 L}{\partial\lambda^2}+\lambda\frac{\partial L}{\partial\lambda}+\left(A+2R\lambda-p^2\lambda^2\right)L=0$$
$$(1-\mu^2)\frac{\partial^2 F}{\partial\mu^2}-\mu\frac{\partial F}{\partial\mu}-\left(-A+p^2\mu^2\right)F=0 \tag{C.9}$$

where A is the separation constant.

Now solve each equation.

C.1 μ EQUATION

Using the substition $\mu = \cos x$, $d\mu = -\sin x dx$, we get the other form of the equation:

$$\frac{dF}{d\mu}=-\frac{1}{\sin x}\frac{dM}{dx} \tag{C.10}$$

$$\frac{d^2F}{d\mu^2}=\frac{d}{dx}\left(-\frac{1}{\sin x}\frac{dM}{dx}\right)\frac{dx}{d\mu}=\frac{d}{dx}\left(-\frac{1}{\sin x}\frac{dM}{dx}\right)\left(-\frac{1}{\sin x}\right)=\left[-\frac{\cos x}{\sin^2 x}\frac{dM}{dx}+\frac{1}{\sin x}\frac{d^2M}{dx^2}\right]\frac{1}{\sin x}\Rightarrow$$
$$\frac{d^2F}{d\mu^2}=\frac{1}{\sin^2 x}\frac{d^2M}{dx^2}-\frac{\cos x}{\sin^3 x}\frac{dM}{dx} \tag{C.11}$$

Plug in equation for $F(\mu)$.

$$\frac{d^2M}{dx^2} - \frac{\cos x}{\sin x}\frac{dM}{dx} + \frac{\cos x}{\sin x}\frac{dM}{dx} + \left(-A + p^2\cos^2 x\right) M = 0 \Rightarrow$$
$$\frac{d^2M}{dx^2} + \left(-A + p^2\cos^2 x\right) M = 0 \tag{C.12}$$

Using $\cos(2x) = \cos^2 x - \sin^2 x = 2\cos^2 x - 1$ we get:

$$\frac{d^2M}{dx^2} + \left[-A + \frac{p^2}{2} + \frac{p^2}{2}\cos(2x)\right] M = 0 \tag{C.13}$$

C.2 λ EQUATION

So assume the solution as the sum of Laguerre polynomials and Algebra:

$L(x) = e^{-px}\sum_{k=0}^{\infty} c_k\, L_k(x)$ with: (the prime is a derivative)

$$x\, L_k^{'}(x) = k\, L_k(x) - k\, L_{k-1}(x)$$
$$x\, L_k^{''}(x) = (x-1)L_k^{'}(x) - k\, L_k(x) = xL_k^{'}(x) - L_k^{'}(x) - n = k\, L_k(x) = \tag{C.14}$$
$$= k\, L_k(x) - k\, L_{k-1}(x) - L_k^{'}(x) - k\, L_k(x) = -L_k^{'}(x) - k\, L_{k-1}(x)$$

First, we shift the domain $\lambda = x + 1$. The equation is:

$$x(x+2)\frac{d^2\, L}{d\, x^2} + (x+1)\frac{d\, L}{d\, x} + \left[-p^2x^2 - 2p^2x + 2Rx - p^2 + 2R - A\right] L = 0; \tag{C.15}$$

And the derivatives are:

$$L^{'} = -p\, e^{-px} \sum_{k=0}^{\infty} c_k\, L_k + e^{-px} \sum_{k=0}^{\infty} c_k\, L_k^{'}$$
$$L^{''} = p^2 e^{-px} \sum_{k=0}^{\infty} c_k\, L_k - 2pe^{-px} \sum_{k=0}^{\infty} c_k\, L_k^{'} + e^{-px} \sum_{k=0}^{\infty} c_k\, L_k^{''} \tag{C.16}$$

Now plug in the L equation:

$$x(x+2)p^2 e^{-px} \sum_{k=0}^{\infty} c_k\, L_k - 2x(x+2)p\, e^{-px} \sum_{k=0}^{\infty} c_k\, L_k^{'} + x(x+2)e^{-px} \sum_{k=0}^{\infty} c_k\, L_k^{''} -$$
$$-(x+1)p\, e^{-px} \sum_{k=0}^{\infty} c_k\, L_k + (x+1)e^{-px} \sum_{k=0}^{\infty} c_k\, L_k^{'} +$$
$$+\left[-p^2x^2 + (-2p^2+2R)x - p^2 + 2R\right] e^{-px} \sum_{k=0}^{\infty} c_k\, L_k = -Ae^{-px} \sum_{k=0}^{\infty} c_k\, L_k \tag{C.17}$$

Cancel exponential and p^2 terms:

$$-2(x+2)p \sum_{k=0}^{\infty} c_k\, xL_k^{'} + (x+2) \sum_{k=0}^{\infty} c_k\, xL_k^{''} - p \sum_{k=0}^{\infty} c_k\, xL_k - p \sum_{k=0}^{\infty} c_k\, L_k +$$
$$+\sum_{k=0}^{\infty} c_k\, xL_k^{'} + \sum_{k=0}^{\infty} c_k\, L_k^{'} + 2R \sum_{k=0}^{\infty} c_k\, xL_k + \left(-p^2 + 2R\right) \sum_{k=0}^{\infty} c_k\, L_k = -A \sum_{k=0}^{\infty} c_k\, L_k \tag{C.18}$$

Expand the derivatives

$$-2(x+2)p \sum_{k=0}^{\infty} c_k\, k\, L_k + 2(x+2)p \sum_{k=0}^{\infty} c_{k-1}\, k\, L_{k-1} - (x+2) \sum_{k=0}^{\infty} c_k\, L_k^{'} - (x+2) \sum_{k=0}^{\infty} c_{k-1}\, k\, L_{k-1} -$$
$$-p \sum_{k=0}^{\infty} c_k\, xL_k - p \sum_{k=0}^{\infty} c_k\, L_k + \sum_{k=0}^{\infty} c_k\, k\, L_k - \sum_{k=0}^{\infty} c_{k-1}\, k\, L_{k-1} + \sum_{k=0}^{\infty} c_k\, L_k^{'} + 2R \sum_{k=0}^{\infty} c_k\, xL_k +$$
$$\left(-p^2 + 2R\right) \sum_{k=0}^{\infty} c_k\, L_k = -A \sum_{k=0}^{\infty} c_k\, L_k$$

(C.19)

Expand again:

$$-2p\sum_{k=0}^{\infty}c_k\,k\,xL_k-4p\sum_{k=0}^{\infty}c_k\,k\,L_k+2p\sum_{k=0}^{\infty}c_{k-1}\,k,x\,L_{k-1}+4p\sum_{k=0}^{\infty}c_{k-1}\,k\,L_{k-1}-\sum_{k=0}^{\infty}c_k\,k\,L_k+\sum_{k=0}^{\infty}c_{k-1}\,k$$

$$-2\sum_{k=0}^{\infty}c_k\,L_k^{'}-\sum_{k=0}^{\infty}c_{k-1}\,k\,x\,L_{k-1}-2\sum_{k=0}^{\infty}c_{k-1}\,k\,L_{k-1}-p\sum_{k=0}^{\infty}c_k\,xL_k-p\sum_{k=0}^{\infty}c_k\,L_k+\sum_{k=0}^{\infty}c_k\,k\,L_k-\sum_{k=0}^{\infty}c_{k-1}$$

$$+\sum_{k=0}^{\infty}c_k\,L_k^{'}+2R\sum_{k=0}^{\infty}c_k\,xL_k+\left(-p^2+2R\right)\sum_{k=0}^{\infty}c_k\,L_k=-A\sum_{k=0}^{\infty}c_k\,L_k \tag{C.20}$$

Group by x, n, etc..:

$$-2p\sum_{k=0}^{\infty}c_k\,k\,xL_k+(2p-1)\sum_{k=0}^{\infty}c_{k-1}\,k\,x\,L_{k-1}-4p\sum_{k=0}^{\infty}c_k\,k\,L_k+(4p-2)\sum_{k=0}^{\infty}c_{k-1}\,k\,L_{k-1}-$$

$$-\sum_{k=0}^{\infty}c_k\,L_k^{'}+(2R-p)\sum_{k=0}^{\infty}c_k\,xL_k+\left(-p^2-p+2R\right)\sum_{k=0}^{\infty}c_k\,L_k=-A\sum_{k=0}^{\infty}c_k\,L_k \tag{C.21}$$

Now use these formulas (from here `http://mathworld.wolfram.com/AssociatedLaguerrePolync`

lines 14 and 16)

$$\frac{d}{d\,x}L_k(x)=-\sum_{i=0}^{k-1}L_i(x) \tag{C.22}$$

we also need this

(from: `http://www.maths.uq.edu.au/MASCOS/Orthogonal09/Warnaar.pdf`):

$$
\begin{aligned}
x\,L_k &= (2k+1)L_k - (k+1)L_{k+1} - k\,L_{k-1} \\
x\,L_{k+1} &= (2k+3)L_{k+1} - (k+2)L_{k+2} - (k+1)\,L_k \\
x\,L_{k-1} &= (2k-1)L_{k-1} - k\,L_k - (k-1)\,L_{k-2} \\
x\,L_{k-2} &= (2k-3)L_{k-2} - (k-1)\,L_{k-1} - (k-2)\,L_{n-3}
\end{aligned}
\tag{C.23}
$$

And plug in again

$$
\begin{aligned}
&\sum_{k=0}^{\infty} c_k \sum_{i=0}^{k-1} L_i(x) - 2p \sum_{k=0}^{\infty} k(2k+1)c_k L_k + 2p \sum_{k=0}^{\infty} k(k+1)c_{k+1}L_{k+1} + 2p \sum_{k=0}^{\infty} k^2 c_{k-1}L_{k-1} + \\
&+ (2p-1) \sum_{k=0}^{\infty} c_{k-1}\,k(2n-1)L_{k-1} - (2p-1) \sum_{k=0}^{\infty} c_k\,k^2 L_k - (2p-1) \sum_{k=0}^{\infty} c_{k-2}\,k(k-1)L_{k-2} - \\
&- 4p \sum_{k=0}^{\infty} c_k\,k\,L_k + (4p-2) \sum_{k=0}^{\infty} c_{k-1}\,k\,L_{k-1} + (2R-p) \sum_{k=0}^{\infty} c_k\,(2k+1)L_k - (2R-p) \sum_{k=0}^{\infty} c_{k+1}\,(k+1)L_k \\
&- (2R-p) \sum_{k=0}^{\infty} c_{k-1}\,k\,L_{k-1} + \left(-p^2 - p + 2R\right) \sum_{k=0}^{\infty} c_k\,L_k = -A \sum_{k=0}^{\infty} c_k\,L_k
\end{aligned}
\tag{C.24}
$$

Now group by n and for clarity remove the sum and c_k terms:

$$\sum_{k=0}^{\infty} c_k \left\{ \sum_{i=0}^{k-1} L_i(x) + \right.$$

$$+ \left[-2pk(2k+1) - (2p-1)k^2 - 4pk + (2R-p)(2k+1) - p^2 - p + 2R \right] L_k +$$

$$+ \left[2pk(k+1) - (2R-p)(k+1) \right] L_{k+1} +$$

$$+ \left[2pk^2 + (2p-1)k(2k-1) + (4p-2)k - (2R-p)k \right] L_{k-1} -$$

$$\left. - \left[(2p-1)k(k-1) \right] L_{k-2} \right\} \tag{C.25}$$

Now multiply by $L_m(x)$ and use the orthogonality of Laguerre's polynomials. The result is an 'almost' lower triangual matrix, called Hessenberg matrix.

//TODO:Remove Once the value of k has been estimated, the vibrational energy levels are:

$$E_n = \hbar \left(n + \frac{1}{2} \right) \sqrt{\frac{k}{m}} \tag{C.26}$$

APPENDIX D

FORTRAN CODE FOR CALCULATING ENERGIES FOR THE 2D PROBLEM

To run the numerical calculations I used gfortan 5.2.0, running on 2.2 GHz, Intel Code 7, Macbook Pro 15" Laptop (mid 2014). The numerial library used was Lapack, version 3.6.0, compiled on the same machine using the gfortran above.

This is Fortran 90 code for calculating even and odd eigenvalues and consequently the energies.

```
! To Compile
! gfortran -O4 -o h2Plus h2plus.f90 hpsort.f90 -L ./ -l lapacke -l lapack -l blas -l
program main

implicit none

interface
```

```
subroutine M_Matrix(mMatrix,max,p)
integer :: max
double precision :: p
double precision,dimension(:,:) :: mMatrix
end subroutine

subroutine L_Matrix(lMatrix,max,R,p)
integer :: max
double precision :: R,p
double precision,dimension(:,:) :: lMatrix
end subroutine

subroutine CalculateEigenvalues(c,matrix,max,wr,wi)
character*1 :: c
double precision,dimension(:,:) :: matrix
integer :: max,np,count
double precision,dimension(:) :: wr,wi
end subroutine

subroutine hpsort(n,rra)
integer :: n
double precision, dimension(:) :: rra
```

```
end subroutine


end interface


! Declare local variables
integer,parameter :: max = 500   ! matrix dimesions
integer,parameter :: np = 1000  ! number of p points
integer,parameter :: state = 0   ! 0=ground state, 1=1st excited, etc..
integer,parameter :: numRadii = 1
double precision,dimension(numRadii) :: Radii
double precision,dimension(max,max) :: mMatrix,lMatrix
double precision,dimension(np) :: pGrid
double precision :: R  ! Nuclei distance
double precision,dimension(max,np) :: mEig, lEig
double precision,dimension(max) :: wr,wi
double precision :: pStep, pMin, pMax
integer :: count,i,j, index
double precision :: p,rr
character(len=6) :: fmt
character(len=16) :: rOut


i = 1;
rr = 20.0d0
```

```
do while( (rr <= 5.0d0) .and. (i <= numRadii))
Radii(i) = rr
  rr = rr + 0.2d0
i = i + 1
end do

do while(i <= numRadii)
  Radii(i) = rr
rr = rr + 0.5d0
  i = i + 1
end do

do j = 1, numRadii
R = Radii(j)

print *,"R = ", R

pMin = 0
pMax = 2.d0*R + 1.d0
pStep = (pMax - pMin) / dble(np)

count = 1;
p = pMin
```

```
do while( count <= np )
! Initialize M  matrix
call M_Matrix(mMatrix,max,p)

!Calculate eigenvalues for M matrirx
call CalculateEigenvalues('m',mMatrix,max,wr,wi)
   !  sort
do i = 1,max
if( wi(i) /= 0) then
wr(i) = -1.0d99
end if
end do

call hpsort(max,wr)
do i = 1,max
mEig(i,count) = wr(max-i+1)
end do

! And L Matrix
call L_Matrix(lMatrix,max,R,p)
call CalculateEigenvalues('l',lMatrix,max,wr,wi)
do i = 1,max
if( wi(i) /= 0) then
```

```
wr(i) = 1.0d99
end if
end do
call hpsort(max,wr)
   ! wr contains eigenvalues from largest to smallest
do i = 1,max
lEig(i,count) = wr(i)
end do

pGrid(count) = p
p = p + pStep
count = count + 1
end do

! Now write the eigenvalues to file
if( R < 10.0d0 ) then
fmt = "(F3.1)"
else
fmt = "(F4.1)"
end if
write(rOut, fmt) R
open(unit=11,file="Eigenvalues-Even-M-R="//trim(rOut)//".dat")
open(unit=12,file="Eigenvalues-Even-L-R="//trim(rOut)//".dat")
```

```
!  Todo: Excited states
index = 1
do i=1,np
write(11,*) pGrid(i), mEig(1,i),mEig(2,i), mEig(3,i), mEig(4,i), mEig(5,i)
write(12,*) pGrid(i), lEig(1,i),lEig(2,i), lEig(3,i), lEig(4,i), lEig(5,i)
end do
close(11)
close(12)
end do

end  ! main

subroutine CalculateEigenvalues(id,matrix,max,wr,wi)
! Calculate and return the eigenvalues
implicit none

character*1 ::id
double precision,dimension(:,:) :: matrix
integer :: max
double precision,dimension(:) :: wr,wi
!local
double precision,dimension(max,max) :: z
double precision,dimension(:), allocatable :: work
```

```
integer :: info,i
double precision,dimension(1,1) :: dummy
integer :: lda,lwork
double precision :: temp

lda = max
lwork = max * 11

allocate( work(lwork) )

call DGEEV('N','N',max,matrix,lda,wr,wi,dummy,1,dummy,1,work,lwork,info)

deallocate(work)

if( info /= 0 ) then
print *, "Error in info , info = ", info
call exit(1)
end if

end subroutine

subroutine M_Matrix(mMatrix,max,p)
! create the M matrix
```

```
implicit none
interface
   function Delta(m,k)
     double precision :: Delta
     integer, intent(in) :: m,k
   end function Delta
end interface

integer :: max
double precision :: p, val
  double precision,dimension(:,:) :: mMatrix
integer :: m,k

do m = 0,max-1
  do k = 0,max-1
!     Even state
val = ( (-1)*((2.0d0 * k)**2) + ( (p**2.0)/2.0d0) ) * Delta(m,k) + &
!     For the Odd state use
!     val = ( (-1)*((2.0d0 * k + 1)**2) + ( (p**2.0)/4.0d0) ) * Delta(m,k) + &
      ( (p**2)/4.0d0 ) * ( Delta(m,k+1) + Delta(m,k-1) )
mMatrix(m+1,k+1) = val
end do
end do
```

```
!     Even state
mMatrix(1,2) = 2 * mMatrix(1,2)
!     For the Odd state use
! mMatrix(1,1) = -1 + (p**2.)/4.0d0

end subroutine

subroutine L_Matrix(lMatrix,max,R,p)
! create the L matrix
implicit none
interface
   function Delta(m,k)
     double precision :: Delta
     integer, intent(in) :: m,k
   end function Delta

  function SubSum(m,k)
      double precision :: SubSum
      integer, intent(in) :: m,k
   end function SubSum
end interface
```

```
integer :: max
double precision :: p,R,val
double precision, parameter :: PI = 3.14159265358979323846264 3d0
  double precision,dimension(:,:) :: lMatrix
integer :: m,k

do m = 0,max-1
do k = 0,max-1
      val = ((-2.d0)*p*k*(2*k+1) - (2*p-1)*(k**2) - 4*p*k + &
(2*R-p)*(2*k+1)-p -(p**2)+2*R) * Delta(m,k) + &
      (2*p*k*(k+1) - (2*R-p)*(k+1))*Delta(m,k+1) + &
      (2.0d0*p*(k**2) + (2.0d0*p - 1)*k*(2.0d0*k - 1) +(4.0d0*p - 2)*k-&
(2*R - p)*k)*Delta(m,k-1) - &
      (2.0d0*p - 1)*k*(k - 1)*Delta(m,k-2) + SubSum(m,k)
lMatrix(m+1,k+1) = (-1)*val
end do
end do

end subroutine

function SubSum(m,k)
implicit none
interface
```

```
   function Delta(m,k)
     double precision :: Delta
     integer, intent(in) :: m,k
   end function Delta
end interface

double precision :: SubSum
integer, intent(in) :: m,k
integer :: i

SubSum = 0.0d0

do i = 0,k-1
   SubSum = SubSum + Delta(m,i)
end do

end function SubSum

function Delta(m,n)
implicit none
double precision :: Delta
integer, intent(in) :: m,n
```

```
if (m == n) then
    Delta = 1.d0
else
    Delta = 0.d0
end if
end function Delta
```

APPENDIX E

RADIATIVE QUENCHING

```
(* Radiative Quenching *)

(* All values in atomic units *)
(*electron mass *)
m_e = 1;
(* Proton Mass *)
m_p = 1836;
(* Reduced Mass *)
m_μ = m_p / 2;
ħ = 1;
(*SpeedOfLight *)
c = 137 ;
(* Boltzman constant *)
k_B = 3.167*^-6 ;

(* Compute the eigenvalues A, p from the system of equations *)
(* RawData format R, p, A, E, E + 1/R *)
SetDirectory[NotebookDirectory[]];
vS1RawData = Import["./s1_state.mat"][[1]];
vS2RawData = Import["./s2_state.mat"][[1]];
vP2PlusRawData = Import["./p2uPlus_state.mat"][[1]];
vP2MinusRawData = Import["./p2uMinus_state.mat"][[1]];

vS1Data = Table[{vS1RawData[[i]][[1]], vS1RawData[[i]][[5]]}, {i, 1, Length[vS1RawData]}];
vS2Data = Table[{vS2RawData[[i]][[1]], vS2RawData[[i]][[5]]}, {i, 1, Length[vS2RawData]}];
vP2PlusData = Table[
   {vP2PlusRawData[[i]][[1]], vP2PlusRawData[[i]][[5]]}, {i, 1, Length[vP2PlusRawData]}];
vP2MinusData = Table[{vP2MinusRawData[[i]][[1]], vP2MinusRawData[[i]][[5]]},
   {i, 1, Length[vP2MinusRawData]}];

lastR = vS1Data[[Length[vS1Data]][[1]] + 1;

(* Extrapolate to R = 10 *)
vS1Data =
  Join[vS1Data, Table[{i, vS1Data[[Length[vS1Data]][[2]]}, {i, lastR, 10, 1}]];
vS2Data = Join[vS2Data, Table[{i, vS2Data[[Length[vS2Data]][[2]]}, {i, lastR, 10, 1}]];
vP2PlusData = Join[vP2PlusData,
   Table[{i, vP2PlusData[[Length[vP2PlusData]][[2]]}, {i, lastR, 10, 1}]];
vP2MinusData = Join[vP2MinusData,
   Table[{i, vP2MinusData[[Length[vP2MinusData]][[2]]}, {i, lastR, 10, 1}]];
```

```
(* 1sg state, potential curve *)
vs1 = Interpolation[
   Transpose[{vS1Data[[All, 1]], vS1Data[[All, 2]]}], InterpolationOrder → 3];
(* 2sg state, potential curve *)
vs2 = Interpolation[
   Transpose[{vS2Data[[All, 1]], vS2Data[[All, 2]]}], InterpolationOrder → 3];
(* 2P+ state *)
vp2p = Interpolation[
   Transpose[{vP2PlusData[[All, 1]], vP2PlusData[[All, 2]]}], InterpolationOrder → 3];
(* 2sg state, potential curve *)
vp2m = Interpolation[Transpose[{vP2MinusData[[All, 1]], vP2MinusData[[All, 2]]}],
   InterpolationOrder → 3];


limit = 5;
Plot[{vs1[r], vs2[r], vp2p[r], vp2m[r]},
 {r, 0.2, limit}, PlotLabels → Automatic, PlotRange → {5, -4}]


(* Compute the Dipole momement D(r) for the single value of R *)
singleDR[r_, p1_, a1_, p2_, a2_, limit_] :=
 Module[{lSol1, mSol1, lSol2, mSol2, norm1, norm2, dInt, ll1, ll2, mm1, mm2},
  (* 1st wavefunction *)
  (* x = λ, y = μ **)
  lSol1 = NDSolve[{(λ^2 - 1) L''[λ] + λ * L'[λ] + (a1 + 2 r λ - p1^2 λ^2) L[λ] == 0 ,
      L[1.00001] == 0, L'[1.00001] == 1 }, L[λ], {λ, 1.00001, limit}][[1]];
  mSol1 = NDSolve[{(1 - μ^2) M''[μ] - μ * M'[μ] - (a1 + p1^2 μ^2) M[μ] == 0,
      M[0] == 1, M'[0] == 0}, M[μ], {μ, -.99999, .99999}][[1]];
  (* 2nd wavefunction *)
  lSol2 = NDSolve[{(λ^2 - 1) L''[λ] + λ * L'[λ] + (a2 + 2 r λ - p2^2 λ^2) L[λ] == 0 ,
      L[1.00001] == 0, L'[1.00001] == 1}, L[λ], {λ, 1.00001, limit}][[1]];
  mSol2 = NDSolve[{(1 - μ^2) M''[μ] - μ * M'[μ] - (a2 + p2^2 μ^2) M[μ] == 0,
      M[0] == 0, M'[0] == 1}, M[μ], {μ, -.99999, .99999}][[1]];

  (* To evaluate NDSolve output at a single point *)
  ll1[x_] := L[λ] /. lSol1 /. λ → x;
  ll2[x_] := L[λ] /. lSol2 /. λ → x;
  mm1[y_] := M[μ] /. mSol1 /. μ → y;
  mm2[y_] := M[μ] /. mSol2 /. μ → y;

  (* Compute <ψ|ψ> = <ψ1s|ψ1s> + <ψ2s|ψ2s> *)
  (* <ψ1s|ψ1s> *)
```

```
  norm1 = NIntegrate[Conjugate[(L[λ] /. lSol1) (M[μ] /. mSol1)] (L[λ] /. lSol1)
      (M[μ] /. mSol1), {μ, -.99999, .99999}, {λ, 1.00001, limit}];
  (* <ψ2s|ψ2s> *)
  norm2 = NIntegrate[Conjugate[(L[λ] /. lSol2) (M[μ] /. mSol2)] (L[λ] /. lSol2)
      (M[μ] /. mSol2), {μ, -.99999, .99999}, {λ, 1.00001, limit}];
  dInt = (r/2) 1/Sqrt[norm1 + norm2] (
      (mm1[-0.99999] × mm2[-0.99999] + mm1[0.99999] × mm2[0.99999]) NIntegrate[
         Conjugate[(L[λ] /. lSol1)] λ (L[λ] /. lSol2), {λ, 1.00001, limit}] +
       NIntegrate[
        Conjugate[(M[μ] /. mSol1)] μ (M[μ] /. mSol2), {μ, -0.99999, 0.99999}]
    );
  {r, (-1) dInt - r }
 ]


GetInputData[state1_, state2_] := Module[{inputData, deltaV},
   Switch[state1,
    "s1",
        Switch [state2,
         "p+",
             deltaV[r_] := Abs[vs1[r] - vp2p[r]];
             inputData = Transpose[
               {vS1RawData[[All, 1]], vS1RawData[[All, 2]],
        vS1RawData[[All, 3]], vP2PlusRawData[[All, 2]], vP2PlusRawData[[All, 3]]}],
         "p-",
             deltaV = Abs[vs1[r] - vp2m[r]];
             inputData = Transpose[
               {vS1RawData[[All, 1]], vS1RawData[[All, 2]], vS1RawData[[All, 3]],
        vP2MinusRawData[[All, 2]], vP2MinusRawData[[All, 3]]}],
         _, Throw["Invalid State"]],
    "s2",
        Switch [state2,
         "p+",
             deltaV[r_] := Abs[vs2[r] - vp2p[r]];
             inputData = Transpose[
               {vS2RawData[[All, 1]], vS2RawData[[All, 2]],
        vS2RawData[[All, 3]], vP2PlusRawData[[All, 2]], vP2PlusRawData[[All, 3]]}],
         "p-",
             deltaV = Abs[vs2[r] - vp2m[r]];
             inputData = Transpose[
               {vS2RawData[[All, 1]], vS2RawData[[All, 2]], vS2RawData[[All, 3]],
        vP2MinusRawData[[All, 2]], vP2MinusRawData[[All, 3]]}],
```

```
        _, Throw["Invalid State"]],
     _, Throw["Invalid State"]];
    {inputData, deltaV}
   ];

{inputDataPlus, deltaV} = GetInputData["s1", "p+"];
{inputDataMinus, deltaV} = GetInputData["s1", "p-"];
```

In[ ]:=

```
CalcDR[inputData_, limit_] := Module[{allDR, dR},
   allDR = Map[singleDR[#[[1]], #[[2]], #[[3]], #[[4]], #[[5]], limit] &, inputData];
    dR = Interpolation[
     Transpose[{allDR[[All, 1]], allDR[[All, 2]]}], InterpolationOrder → 3];
     dR
   ];

dRPlus = CalcDR[inputDataPlus, limit];
dRMinus = CalcDR[inputDataMinus, limit];
```

In[ ]:=

```
(*Plot[{dRPlus[r],dRMinus[r]},{r,.2,5}, PlotLabels→{"2p+ -> 1s+","2p+ -> 1s+"},
 Frame→True,FrameLabel→{"R (units of a_u)", "D(R) (units of a_u}"} ]*)
Plot[{dRPlus[r]}, {r, .2, 5},  Frame → True,
 FrameLabel → {"R (units of a_u)", "D(R) (units of a_u}"} ]
```

```
aR[x_, state1_, state2_, limit_] := Module[{inputData, deltaV, dR, dV},
   {inputData, dV} = GetInputData[state1, state2];
   dR = CalcDR[inputData, limit];
   deltaV[r_] := dV[r];
   4/3 (dR[x])^2 (deltaV[x])^3/c^3
  ];
```

```
(* Energy  Range, for temperatures from 0K - 2K
   k_B T = 1/2 m v^2 = E, t in Kelvin  *)

energies = Interpolation[ Table[k_B t, {t, 0, 20, .5}], InterpolationOrder → 3];
k_a[r_] := Sqrt[2 m_μ (energies[r] - v_s1[10])];


solF[j_] := Sort[Transpose[NDEigensystem[
       1/r D[r D[ff[r], r], r] - (v_s1[r] + j^2/r^2) ff[r], ff, {r, 0.2, limit}, 5,
       Method → {"SpatialDiscretization" →
          {"FiniteElement", {"MeshOptions" → {MaxCellMeasure → 0.001}}}}]]][[1]];


(* 2D Schrodinger equation, m is a paramete #  (called J in 3D),
grab the lowest eigenvalue, i.e. value of k *)
solS1J = Sort[Transpose[NDEigensystem[
        1/r D[r D[ff[r], r], r] - (v_s1[r] + #^2/r^2) ff[r], ff, {r, 0.2, limit}, 5,
        Method → {"SpatialDiscretization" →
           {"FiniteElement", {"MeshOptions" → {MaxCellMeasure → 0.001}}}}]]][[1]] &;
(*solS2J[j_]:=Sort[Transpose[
    NDEigensystem[1/r D[r D[ff[r],r],r] -(v_s2[r]+j^2/r^2) ff[r],ff[r],{r,0.2, limit}, 5,
     Method→{"SpatialDiscretization"→
        {"FiniteElement",{"MeshOptions"→{MaxCellMeasure→0.001}}}}]]];*)
(* Here m = 0 for 1S state *)
allS1Js = Map[solS1J, Table[i, {i, 0, 0}]];
allS1Ks =  allS1Js[[All, 1]];
allS1JFunc = allS1Js[[All, 2]] ;
k_a = allS1Ks[[1]]

fS1[j_, x_] := allS1JFunc[[j]][x];

(* Calculate the integral *)

 η_s1pp[j_] := NIntegrate[(Abs[ fS1[j,x]])^2 aR[x,"s1", "p+", limit],{x,.2,limit}];
ScientificForm[η_s1pp[1]]
```

```
ηs1pm[j_] :=
  NIntegrate[(Abs[ allS1JFunc[[j]][x] ])^2 aR[x, "s1", "p-", limit], {x, .2, limit}];

ηs2pp[j_] :=
  NIntegrate[(Abs[allS2JFunc[[j]][x]])^2 aR[x, "s2", "p+", limit], {x, .2, limit}];

ηs2pm[j_] :=
  NIntegrate[(Abs[allS2JFunc[[j]][x]])^2 aR[x, "s2", "p-", limit], {x, .2, limit}];


(* Cross Section *)

σ = Π/kA^2 Sum[1 - Exp[-4 ηspp[j]], {j, 1, 10}];
σ
```

BIBLIOGRAPHY

[1] various authors. Quantum information processing. https://link.springer.com/journal/11128.

[2] F. Jazaeri, A. Tajalli A. Beckers, and J. Sallese. A review on quantum computing: From qubits to front-end electronics and cryogenic mosfet physics. 2019.

[3] Colin D. Bruzewicz, John Chiaverini, Robert McConnell, and Jeremy M. Sage. Trapped-ion quantum computing: Progress and challenges. *Applied Physics Reviews*, 6(2):021314, Jun 2019.

[4] Sandra Das Sarma, Michael Freedmana, and Chetan Nayak. Topological quantum computation. http://stationq.cnsi.ucsb.edu/~freedman/publications/96.pdf.

[5] Sankar Das Sarma, Michael Freedman, and Chetan Nayak. Topologically-protected qubits from a possible non-abelian fractional quantum hall state. *Phys. Rev. Lett*, 94, 2005.

[6] Robert Raussendorf, Jim Harrington, and Kovid Goyal. Topological fault-tolerance in cluster state quantum computation. *New Journal of Physics*, 9, 2007.

[7] Jiannis K. Pachos. Introduction to topological quantum computation.

[8] Michael Freedman, Alexei Kitaev, Larsen, Michael J., and Zhenghan Wang. Topological quantum computation. *Bulletin of the American Mathematical Society*, 40, 2003.

[9] Andrew J. Mannix, Brian Kiraly, Mark C. Hersam, and Nathan P. Guisinger. Synthesis and chemistry of elemental 2d materials. *Nature Reviews Chemistry 1*, January 2017.

[10] Joseph M. Proud and Lawrence H. Luessen. *Radiative Processes in Discharge Plasmas*. Springer, 1986.

[11] Ady Stern. Anyons and the quantum hall effect - a pedagogical review. *Annals of Physics*, 323, 2008.

[12] L. D. Landau. Zur theorie der phasenumwandlungen ii. *Phys. Z. Sowjetunion*, 11:26–35, 1937.

[13] R. E. Pierls. Quelques proprietes typiques des corpses solides. *Ann. I. H. Poincare*, 5:177–222, 1935.

[14] P. C. Hohenberg. Existence of long-range order in one and two dimensions. *Physical Review Letters*, 153, June 1967.

[15] Mermin N.D. and Wagner H. Absence of ferromagnetism or antiferromagnetism in one- or two-dimensional isotropic heisenberg models. *Phys. Rev. Lett*, 17, November 1966.

[16] J.G.Dash. Two-dimensional matter. *Endeavour*, 6(1):15–22, 1982.

[17] Geim A.K. and Novoselov K.S. The rise of graphene. *Nature Materials*, 2007.

[18] Geim Andre and Novoselov Konstantin. Nobel prize in physics for graphene. `http://www.nobelprize.org/nobel_prizes/physics/laureates/2010/advanced-physicsprize2010.pdf`, 2010.

[19] Mark Bowick and Luca Giomi. Two-dimensional matter: Order, curvature and defects. *Physics.Paper 139*, 2009.

[20] B. Partoens and F.M. Peeters. From graphene to graphite: Electronic structure around the k point. *Phys. Rev. B*, 72, 2005.

[21] Fasolino A., Los J. H., and Katsnelson M. I. Intrinsic ripples in graphene. *Nature Materials*, 6:858–861, 2007.

[22] Dirac P.A.M. The quantum theory of the electron. *Proceedings of the Royal Society A: Mathematical, Physical and Engineering Sciences*, 117, 1928.

[23] A Bostwick, T Ohta, T Seyller, K Horn, and E Rotenberg. Quasiparticle dynamics in graphene. *Nature Physics*, 3, 01 2007.

[24] W Y Liang. Excitons. *Physics Education*, 5:226–228, 1970.

[25] Gregory Wannier. The structure of electronic excitation levels in insulating crystals. *Physical Review*, 52, 1937.

[26] Z.G. Koinov. Excitons in two dimensions: the excitation spectrum and phase transition to superfluidity. *Physics Letters A*, 265:297–303, 2000.

[27] Unuchek D, Ciarrocchi A., Avsar A., and et al. Room-temperature electrical control of exciton flux in a van der waals heterostructure. `https://doi.org/10.1038/s41586-018-0357-y`, 2018.

[28] R Singh. *Excitons in Semiconductor Quantum Wells Studied Using Two-Dimensional Coherent Spectroscopy*. PhD thesis, University of Colorado, Boulder, CO, 2015.

[29] Science Direct. Two-dimensional materials. `https://www.sciencedirect.com/topics/materials-science/two-dimensional-materials`.

[30] various authors. 2d layered materials: From materials properties to device applications. `http://ieeexplore.ieee.org/document/7409780/?reload=true`.

[31] various authors. 2d materials and electronic devices. `http://iopscience.iop.org/journal/0022-3727/page/2D-materials-and-electronic-devices`.

[32] Wu Judy and Weitering Hanno. Superconductivity in 2d materials. https://iopscience.iop.org/journal/0953-2048/page/Focus-on-Superconductivity-in-the-2D-Limit.

[33] Sidney G. Davison and Maria Steslicka. *Basic Theory of Surface States*. Clarendon Press, 1992.

[34] Jason S. Ross, Philip Klement, Aaron M. Jones, Nirmal J. Ghimire, Jiaqiang Yan, D. G. Mandrus, Takashi Taniguchi, Kenji Watanabe, Kenji Kitamura, Wang Yao, David H. Cobden, and Xiaodong Xu. Electrically tunable excitonic light-emitting diodes based on monolayer wse2 p-n junctions. *Nature Nanotechnology*, 9:268–272, 2014.

[35] HQ Graphene. Black phosphorus. http://www.hqgraphene.com/Black-Phosphorus.php.

[36] Yu. Yu. Illarionov, M. Walt, G. Rzepa, T. Knobloch, J.S. Kim, D. Akinwande, and T. Grasser. Highly stable black phosphorus field-effect transistors with low density of oxide traps. https://www.nature.com/articles/s41699-017-0025-3.

[37] Jingsi Qiao, Xianghua Kong, Zhi-Xin Hu, Feng Yang, and Wei Ji. Few-layer black phosphorus: emerging direct band gap semiconductor with high carrier mobility. https://arxiv.org/vc/arxiv/papers/1401/1401.5045v1.pdf.

[38] Stephen Cook. The p versus np problem. https://www.claymath.org/sites/default/files/pvsnp.pdf.

[39] Richard Feynman. Simulating physics with computers. *International Journal of Theoretical Physics*, 21 (6-7):467–488, 1982.

[40] S Garey M. R, Johnson D. Computers and intractability: A guide to the theory of np-completeness, 1972.

[41] Peter W Shor. Polynomial-time algorithms for prime factorization and dis-

crete logarithms on a quantum computer. *SIAM J. Sci. Statist. Comput*, 26:1484–1509, 1997.

[42] Carl Pomerance. Analysis and comparison of some integer factoring algorithms, in computational methods in number theory, part i. *Math. Centre Tract*, 154:89–139, 1982.

[43] Daniel S. Abrams and Seth Lloyd. Nonlinear quantum mechanics implies polynomial-time solution for np-complete problems. *Physical Review Letters*, 81(18), Nov 1998.

[44] Daniel S. Abrams and Seth Lloyd. Quantum algorithm providing exponential speed increase for finding eigenvalues and eigenvectors. *Physical Review Letters*, 83(24), Dec 1999.

[45] P. Wocjan and S. Zhang. Several natural bqp-complete problems. 2006.

[46] Abhilash Ponnath. Difficulties in the implementation of quantum computers. `https://arxiv.org/pdf/cs/0602096.pdf`.

[47] Leinaas J. M and Myrheim J. On the theory of identical particles. *Physical Review Letters*, 49:957–959, 1976.

[48] Frank Wilczek. Quantum mechanics of fractional-spin particles. `http://www.ifi.unicamp.br/~mtamash/f689_mecquant_i/prl49_957.pdf`, 1982.

[49] Daniel Walsh1. A physicist's introduction to topology: Connections to bosons, fermions, and anyons. `http://physics.ucsd.edu/~mcgreevy/s13/final-papers/2013S-215C-Walsh-Daniel.pdf`.

[50] Robert B. Laughlin, Horst L. Stormer, and Daniel C. Tsui. Discovery of a new form of quantum fluid with fractionally charged excitations. `http://www.nobelprize.org/nobel_prizes/physics/laureates/1998/`.

[51] James R. Wootton and Jiannis K. Pachos. Universal quantum computation with abelian anyon models. `http://arxiv.org/pdf/0904.4373v2.pdf`, 2009.

[52] Alexander Fetter. Rapidly rotating bose-einstein condensates. http://www.int.washington.edu/talks/WorkShops/int_05_2b/People/Fetter_A/A_Fetter.pdf.

[53] John Chalker. Geometrically frustrated magnets. https://www-thphys.physics.ox.ac.uk/people/JohnChalker/research/weizmann09.pdf.

[54] Sagar Vijay, Timothy H. Hsieh, and Liang Fu. Majorana fermion surface code for universal quantum computation. *Physical Review X*, 5(4), Dec 2015.

[55] Sujit Manna, Peng Wei, Yingming Xie, Kam Tuen Law, Patrick A. Lee, and Jagadeesh S. Moodera. Signature of a pair of majorana zero modes in superconducting gold surface states. 117(16):8775–8782, 2020.

[56] Chetan Nayak, Steven H. Simon, Ady Stern, Michael Freedman, and Sankar Das Sarma. Non-abelian anyons and topological quantum computation. *Rev. Mod. Phys*, 80, 2008.

[57] J. Frenkel. On the transformation of light into heat in solids. i. *Physical Review*, 37, 1931.

[58] D. R. Bates, Kathleen Ledsham, and A. L. Stewart. Wave function of the hydrogen molecular ion. *Philosophical Transactions of the Royal Society of London. Series A, Mathematical and Physical Sciences*, 246(911):215–240, 1953.

[59] D. R. Bates and T.R. Carson. Exact wave function of heh2+. *Proceedings of the Royal Society of London. Series A, Mathematical and Physical Sciences*, 234(1197):207–217, 1956.

[60] C Slater, John. *Quantum Theory of Molecules and Solids*. McGraw-Hill, 1963.

[61] Allen Lowell Wasserman. *The hydrogen molecule-ion as a superposition of atomic orbitals*. PhD thesis, Iowa State University, 1963.

[62] A Carrington, I R McNab, and C A Montgomerie. Spectroscopy of the hydrogen molecular ion. *Journal Phys. B*, 22:3551–3586, 1989.

[63] Zygelman B., Dalgarno A., Jamieson M. J., and Stancil P. C. Multichannel study of spin-exchange and hyperfine-induced frequency shift and line broadening in cold collisions of hydrogen atoms. *Phys. Rev. A*, 67, April 2003.

[64] Gregory Colarch. *A Gauge Theoretic Treatment of Rovibrational Motion in Diatoms*. PhD thesis, University of Nevada, Las Vegas, Las Vegas, NV, 2012.

[65] C. David Sherrill. The born-oppenheimer approximation. `http://vergil.chemistry.gatech.edu/notes/bo/bo.html`.

[66] LAPACK. Linear algebra package. `http://www.netlib.org/lapack/`.

[67] Walter Gander. Algorithms for the qr-decomposition. `https://www.inf.ethz.ch/personal/gander/papers/qrneu.pdf`.

[68] S. H. Patil. Hydrogen molecular ion and molecule in two dimensions. *Journal of Chemical Physics*, 118(5), 2003.

[69] Willard Miller Jr. and Alexander V Turbiner. Particle in a field of two centers in prolate spheroidal coordinates: integrability and solvability. `http://arxiv.org/abs/1402.3816`.

[70] Kolos W. and Wolniewicz W. Nonadiabatic theory for diatomic molecules and its application to the hydrogen molecule. *Reviews of Modern Physics*, 35:473–483, July 1963.

[71] D.G.W. Parfitt and M.E. Portnoi. The two-dimensional hydrogen atom revisited. *Journal of Mathematical Physics*, 43, 2002.

[72] X. L. Yang, S. H. Guo, and F. T. Chan. Analytic solution of a two-dimensional hydrogen atom. i. non-relativistic theory. `http://journals.aps.org/pra/abstract/10.1103/PhysRevA.43.1186`.

[73] George B. Arfken and Hans J. Weber. *Mathematical Methods for Physicists*. Elsevier, 2005.

[74] NIST Digital Library of Mathematical Functions. Mathieu's equation. http://dlmf.nist.gov/28.

[75] Julio C. Gutierrez-Vega. Theory and numerical analysis of the mathieu functions. http://optica.mty.itesm.mx/pmog/Papers/Mathieu.pdf, 2008.

[76] Jia-Lin Zhu and Jia-Jiong Xiong. Hydrogen molecular ion in two dimensions. *Physical Review B*, 41(17), 1990.

[77] Milton Abramowitz and Irene A Stegun. *Handbook of Mathematical Functions with Formulas, Graphs, and Mathematical Tables*. Dover Publications, 1964.

[78] Y. D Chong. Scattering theory. "http://www1.spms.ntu.edu.sg/~ydchong/teaching/PH4401_00_scattering.pdf".

[79] R. I Lapidus. Quantum mechanical scattering in two dimensions. *American Journal of Physics*, 50, 1982.

[80] A. Z. Devdariani and E. A. Chesnokov. Radiative quenching and excitation of metastable states upon differential scattering of atoms i. uniform quasi-classical theory. *Optics and Spectroscopy*, 99:858–865, December 2005.

[81] A. Z. Devdariani and E. A. Chesnokov. Radiative quenching and excitation of metastable states upon differential scattering of atoms ii. the he(1s12s1)ne molecule. *Optics and Spectroscopy*, 99:866–872, December 2005.

[82] B.Zygelman and A. Dalgarno. Radiative quenching of he(2 s) induced by collisions with ground-state helium atoms. *Phys. Rev. A*, 38, February 1988.

[83] H. R. Reiss. Limitations of gauge invariance. https://www.researchgate.net/publication/235359877_Limitations_of_gauge_invariance.

[84] Walter R Thorson. Theory of slow atomic collisions. i. h2. *The Journal of Chemical Physics*, 42:3878, 1965.

[85] M. Kimura and W. R. Thorson. Molecular-state study of he2+ - h(1s) and h+ - he+(1s) collisions. *Phys. Rev. A*, 24:3019, 1981.

[86] W.R.Thorson and J.B.Delos. Theory of near-adiabatic collisions.i. electron translation factor method. *Phys.Rev.A*, 18:135, 1978.

[87] S Gasiorowicz. *Quantum Physics*. Wiley, 1974.

[88] B. Zygelman, A. Saenz, P. Froelich, S. Jonsell, and A. Dalgarno. Radiative association of atomic hydrogen with antihydrogen at subkelvin temperatures. *PhysicaL Review A*, 63, 2001.

[89] B. Zygelman, A. Dalgarno, M. Kimura, and N. F. Lane. Radiative and nonradiative charge transfer in he++h collisions at low energy. *Physical Review A*, 40, September 1989.

[90] Zygelman, Lucic, Kotochigova, and Hudson. Cold ion-atom chemistry driven by spontaneous radiative relaxation: A case study for the formation of the ybca+ molecular ion. *Journal of Physics B: Atomic, Molecular and Optical Physics*, 47(1), 2013.

[91] Zygelman B, Stancil P.C., and Dalgarno A. Stimulated radiative association of he and h+. *The Astrophysical Journal*, pages 508–151, 1998.

[92] A Wacker. Fermis golden rule.

[93] Stefan Blugel. Scattering theory: Born series. juser.fz-juelich.de/record/20885/files/A2_Bluegel.pdf.

[94] P.M. Morse and H Feshbach. *Methods of Theoretical Physics*. McGraw-Hill, 1953.

CURRICULUM VITAE

PROFILE

Software engineer with over 18+ years experience in Software Engineering, Business to Business applications, Object Oriented design and methodologies. Highly Proficient in C/C++, UNIX and .NET platform. Up to date knowledge of distributed systems, Algorithms, Computational Mathematics, transaction processing, relational database and network engineering. Strong distributed system design, system programming background, excellent knowledge of mission critical applications, networks, protocols.

KEY SKILLS

• Operating Systems: UNIX (Linux, UNIX , Windows .NET, Win32, Embedded Systems

• Methodologies and concepts: Object Oriented analysis and design, Client/Server and N-tier programming, Design of Distributed Systems

• Real life experience of scaling and optimizing large systems, designing for reliability and scalability

• Throughout knowledge of C++, STL programming practices and paradigms. Early adopter of new C++ standards such as C++03, C++11.

• Excellent knowledge of full range of Microsoft technologies, and recent expertise in C# ,.NET, ASP.NET platform and SQL server (complete .NET stack), Excel RTD Server and Excel Extensions

• Deep knowledge and experience with: distributed systems, Web services, concurrent programming, threads, real time programming, embedded systems, TCP/IP and network protocols

• Experience with database theory, database programming, ORACLE 9i and 10g administration, mySQL

• Implemented Classification, Data analytics, Machine Learning solutions, using NumPY, Tensor Flow and Keras

• Theoretical background: Applied Mathematics, software engineering, digital signal processing applications, statistical process analysis, network analysis, Working experience in writing technical design specification, overseeing the development and testing process, and providing a mentorship role to junior developers and interns.

• Knowledge of practical software engineering techniques, such as basic waterfall and incremental, extreme programming and fast prototyping.

• Programming and Development tools: Gnu, SVN, MS Visual Studio, .NET, ATL, PERL, Mason, Various Unix shells, Purify, Quantify, Matlab

PROFESSIONAL EXPERIENCE, Full Time and Consulting

Tableau Software, Seattle, WA 2017-present

Senior Software Engineer

• Implemented Performance improvement of the existing query pipeline

• Participated in the Implemented of classification network for error tracking and prediction • Migrated several server components from Windows to Linux

• General feature development

• Mentored and supported junior team member.

Microsoft Corp., Redmond, WA 2016-2017

Senior Software Engineer

• Refactoring of the current code base

• Design and implementation of the local Cache subsystem

• Improved the current build and deployment process

Rocket Gaming System, Las Vegas, NV 2013-2014

Senior Math Software Engineer - Consulting

• Design and Implementation of the Game algorithms in C++

• Analyze and define the game characteristics, define and implement the mathematical model

• Refactoring, Performance and Usability improvements of the existing software and software modules.

• Programming the Game simulations of the game math models in C++ and C#.

• Improved the current methodology and development process

Bloomberg Inc, New York, NY 2012-2013

Senior Software Engineer

• Lead the design and implementation of custom Excel function handling high frequency sell side trading and data flow. The application consists of C++ TD server, and C#/.NET Excel UI extension.

• Designed and implemented the data flow, algorithms and Excel UI for the Bloomberg specific financial functions.

• Worked with other teams to implement end to end, high frequency trading and data flow applications. The applications are the real time Excel exten-

sions, passing large data sets to customer trading models, and executing customers orders in real time.

• Performance improvement, refactoring of existing applications,

Translattice, Santa Clara. CA 2010 – 2011

Senior Software Engineer

• Implementation of the Paxos algorithm for distributed DB operation on Postgres DB engine in C.

• Design and Implementation of distributed transactions, distributed table sharding for the Postgres DB

• Design and Implementation of the underlying multithreaded and multi process communication / replication functionality.

• Performance improvements, refactoring existing code, Using C for the database engine and C++ for the tools.

MySpace.com, Seattle, WA 2007 – 2010

Senior Software Engineer/Architect

• Lead the design and implementation of MySpace Messaging system, which included internal messaging and email server and client. The project integrated new messaging, email, comments, WebIm into the existing MySpace framework. Project was based on .NET platform, using C#, ASP.NET, SQL Server . • Designed and developed message passing system supporting transaction like operation.

• Developed Rest based services, using full .NET stack, from SQL Server as a back end DB to the C#/.NET as middle tier.

• Significantly refactored and the existing design, to provide the transition path to the new architecture

• Engineered and implemented the Web Service interoperability solutions between MySpace back end systems and external partners.

• Providing the design for the transition to multi level application, highly scalable system.

textbfAmazon.com. Seattle, WA 2004 – 2007

Senior Software Engineer (III)

• Leading the design of the next generation high performance, distributed software deployment system.

• Designed and developed (as a lead in the team) distributed and multithread set of C++ applications to effectively manage, update and monitor over 30,000+ hosts. The whole system consisted of several server side applications, each on separate server farm, set of client apps and daemons, persistence subsystem (Database) and a data streaming subsystem. The amount of data stored was second only to customer data within Amazon.

• Used several C++ libraries, multithread, multiprocessing methodologies and applications Justified and implemented specific solutions, related to scaling, performance improvement, operational support of the software configuration, distribution and release management

• Developed and programmed on the application server stack, from database (Oracle 9i and 10g) to application servers, Web servers, end host tools

• Improved, refactored, and significantly increased functionality of the existing application by improving performance, availability and usability

• Lead a team, provided designed review, support to junior team members

textbfPACKETEER Inc., Kelowna, BC 2002 – 2004

Software Engineer

• Implementation of compression algorithms for IP, TCP and HTTP based traffic in C.

• Member of the design and team for of the next generation TCP traffic-processing server. The application was developed in C for kernel drivers and C++ for the higher layers.

• Linux network stack programming and customization in C.

• Implementation of algorithm for traffic classification, supporting XML and SOAP protocols in C++.

• Troubleshooting of network and network based applications.

• Design of performance critical system and application

...

EDUCATION

PhD Physics (Close to completion) University of Nevada Las Vegas, Las Vegas, NV

Master of Applied Mathematics University of Washington, Seattle, WA

Master of Engineering Simon Fraser University, Vancouver, BC, Canada

B.Sc. Hon in Electrical Engineering School of Electrical Engineering, University of Sarajevo